

8-2018

## Geophysical Assessment of Subsurface Soil Conditions Using Capacitively Coupled Resistivity

Folaseye Coker  
*University of Arkansas, Fayetteville*

Follow this and additional works at: <https://scholarworks.uark.edu/etd>



Part of the [Civil Engineering Commons](#), and the [Soil Science Commons](#)

---

### Citation

Coker, F. (2018). Geophysical Assessment of Subsurface Soil Conditions Using Capacitively Coupled Resistivity. *Graduate Theses and Dissertations* Retrieved from <https://scholarworks.uark.edu/etd/2848>

This Thesis is brought to you for free and open access by ScholarWorks@UARK. It has been accepted for inclusion in Graduate Theses and Dissertations by an authorized administrator of ScholarWorks@UARK. For more information, please contact [scholar@uark.edu](mailto:scholar@uark.edu), [uarepos@uark.edu](mailto:uarepos@uark.edu).

Geophysical Assessment of Subsurface Soil Conditions Using Capacitively Coupled  
Resistivity

A thesis submitted in partial fulfillment  
of the requirements for the degree of  
Master of Science in Civil Engineering

by

Folaseye Coker  
University of Oklahoma  
Bachelor of Science in Civil Engineering, 2013

August 2018  
University of Arkansas

This thesis is approved for recommendation to the Graduate Council

---

Clinton M. Wood, PhD  
Thesis Director

---

Michelle Bernhardt, PhD  
Committee Member

---

Sarah Hernandez, PhD  
Committee Member

## **Abstract**

The purpose of this research is to explore the applicability of Capacitively-Coupled Resistivity (CCR) as an improvement on traditional drilling and sampling methods for subsurface soil investigations. The CCR method could be used to identify critical locations for drilling and sampling such as expansive clay layers and anomalies (sinkholes, unknown landfills, etc.) rather than uniformly sampling across a site. CCR surveys were performed at Alpena, Arkansas along a highway expansion project changing US 62 from a two lane to four lane highway, and at Alton, Illinois along the Mel Price Levee, a 5.2 mile levee along a portion of the Mississippi River. A geometrics OhmMapper was used to acquire the CCR resistivity data with emphasis placed on investigating the near surface material properties (0-5 meters). The Alpena site was comprised of silt, clay and suspected bedrock with a deep water table, while the Alton site was comprised of clay and sand with a shallow water table. The survey was performed at both sides of the highway at Alpena and along the landside and riverside of the levee at Alton. The resulting resistivity plots revealed continuous subsurface soil information and emphasizes the impact of water level when interpreting the resistivity results as significant changes in the resistivity ranges for fine and coarse grain soils are possible for different moisture conditions. The measured soil resistivity values at the Alpena site with a deep water table were much higher than the values at the Alton site with the shallow water table. The accuracy of the CCR method was assessed by identifying the number of locations where the soil type predicted by CCR matched the existing boring and CPT logs. Resistivity from CCR was able to distinguish between areas of predominantly fine-grained material and coarse-grained material but limitations exist in separating soils with similar grain sizes (silts and clays).

## Table of Contents

1	Introduction .....	1
2	Literature Review .....	2
2.1	Introduction .....	2
2.2	Capacitively Coupled Resistivity (CCR) .....	2
2.3	Typical Electrical Resistivity Values for Soil .....	4
2.4	Depth of Exploration .....	5
2.5	Previous Research .....	6
2.5.1	Geophysical Characterization of the American River Levees, Sacramento, California, using Electromagnetics, Capacitively Coupled Resistivity, and DC Resistivity.....	6
2.5.2	Using Ground-Penetration Radar And Capacitively Coupled Resistivity To Investigate 3-D Fluvial Architecture And Grain-Size Distribution of A Gravel Flood Plain In North East British Columbia, Canada.....	8
2.6	Other Use of CCR .....	9
2.6.1	Identify Karst Features.....	9
3	Methods and Materials .....	10
3.1	Introduction .....	10
3.2	Capacitively Coupled Resistivity .....	11
3.2.1	General Data Acquisition Methodology .....	12
3.2.2	Data Processing.....	14
3.3	Alpena Testing .....	18

3.4	Mel Price Levee Testing .....	23
4	Results .....	29
4.1	Alpena .....	29
4.2	Mel Price Levee .....	35
4.2.1	Landside .....	35
4.2.2	Riverside .....	38
4.2.3	Comparison between Resistivity Results .....	41
5	Conclusion .....	42
6	References .....	43

## Table of Figures

Figure 2-1. The OhmMapper system shown with five receiver dipoles and the transmitter dipole towed by an all-terrain vehicle (Lucius et al. 2008) .....	3
Figure 2-2. A schematic of the OhmMapper capacitively coupled AC resistivity system with one transmitter dipole and two receiver dipoles arranged in dipole-dipole configuration (Lucius et al. 2008) .....	3
Figure 2-3. Example CCR survey results (Garman and Purcell 2004).....	4
Figure 2-4. OhmMapper configuration with five dipoles and a transmitter (modified from Geometrics 2001) (Hickin et al. 2009) .....	5
Figure 2-5. USGS American River Levee survey OhmMapper and DC resistivity inversion results in 3D (Asch et al. 2007) .....	7
Figure 2-6. Resistivity plots for some sections along the USGS American River Levee survey (Asch et al. 2007).....	7
Figure 2-7. Resistivity Plots Along the Lines Traveled By The OhmMapper. (BR is bar, TL is local topographic low, and FP is undifferentiated floodplain). .....	9
Figure 2-8. Underground resistivity plot based on OhmMapper measurements (Vadillo et al, 2012) .....	10
Figure 3-1. Resistivity Analysis Location at Mel Price Levee and Alpena Highway Alignment .....	11
Figure 3-2. A) Transmitter and Receivers B) Dipole Cables connected to receivers with protective shields at the site. C) Data logger with Trimble Geo 7x GPS device mounted on the All-Terrain Vehicle (ATV) D) OhmMapper setup towed in a line by ATV along US 62 near Alpena, Arkansas. ....	13
Figure 3-3. OhmImager Screen showing the apparent resistivity vs distance plot modeled from data acquired by the OhmMapper. ....	15

Figure 3-4. MagMap Screenshot showing A) before and B) after the resistivity data filter process for spikes and dropouts. .... 16

Figure 3-5. MagMap Screenshot showing resistivity pseudosection along the travel path. .... 16

Figure 3-6. Sample resistivity profile generated by Surfer. .... 18

Figure 3-7. NOAA Station in Springfield Missouri precipitation records from January 2012 to January 2018. .... 20

Figure 3-8. Alpena Highway Alignment showing the start and end positions of the data acquisition process along both sides of the highway conducted using the OhmMapper. Letters in the figure correspond to pictures in Figure 3-10. .... 21

Figure 3-9. AHTD Job 090230 soil boring log for a portion along US 62 highway west of Alpena, AR ..... 22

Figure 3-10. Along the Alpena Highway alignment OhmMapper towed at; A) STA 403+00 right side of highway, B) STA 451+00 passing over a buried utility crossing the highway on the right side, C) STA 484+00 left side of the highway, D) STA 491+00 passing through a gas station on the right side of the highway. .... 23

Figure 3-11. Mel Price Levee showing the start and end positions of the data acquisition process along the landside and riverside of the levee conducted using the OhmMapper. .... 24

Figure 3-12. A) Visible surface water at landside of Mel Price Levee at sta. 123+00, B) View from top of road showing the pond along the landside of the Mel Price Levee at sta 95+00, and C) OhmMapper towed along riverside of Mel Price Levee at sta 82+00. .... 25

Figure 3-13. Soil boring log collected along the landside toe of the Mel Price Levee. .... 26

Figure 3-14. CPT log collected along the riverside toe of the Mel Price Levee. .... 27

Figure 3-15. OhmMapper towed along the top of the Mel Price Levee collecting resistivity data. .... 27

Figure 3-16. Sample subsurface 2D inversion model generated by RES2DINV software. .... 28

Figure 4-1. Resistivity soil profiles along the left and right side of the road at Alpena, Arkansas showing the soil type, station, and boring depth location at the top of the resistivity plot .....	33
Figure 4-2. Relationship between moisture content and resistivity of boring log soil samples collected at the Alpena, Arkansas site. ....	33
Figure 4-3. Relationship between plastic index and resistivity of boring log soil samples collected at the Alpena, Arkansas site. ....	34
Figure 4-4. Relationship between liquid limit and resistivity of boring log soil samples collected at the Alpena, Arkansas site. ....	34
Figure 4-5. a) Distribution of soil samples for various resistivity values and b) Distribution of soil samples either side hypothetical resistivity separator between clay and silt samples based on resistivity at the Alpena site.....	35
Figure 4-6. Resistivity profile from CCR along the landside of Mel Price Levee. ....	37
Figure 4-7. Plot of relationship between plastic index and resistivity of boring log soil samples collected along the landside of the Mel Price Levee. ....	37
Figure 4-8. a) Distribution of soil samples b) Distribution of soil samples either side hypothetical resistivity separator between clay and sand samples based on their resistivity at landside of Mel Price site.....	38
Figure 4-9. Resistivity profile from CCR along the riverside of Mel Price Levee.....	40
Figure 4-10. Relationship between $I_{sbt}$ and resistivity of CPT soil samples collected along the riverside of the Mel Price Levee. Identified soil types are based on $I_{sbt}$ .....	40
Figure 4-11. a) Distribution of soil samples b) Distribution of soil samples either side hypothetical resistivity separator between clay and sand samples based on their resistivity along the riverside of Mel Price Levee. ....	41



## Table of Tables

Table 2-1. Typical resistivity values established by Palacky. 1987, Burger et al. 1992, and Hickin et al. 2008.....	5
Table 3-1 Coordinates showing the location of Capacitively Coupled Resistivity Test sites .	11
Table 3-2. Resistivity Survey Parameters and Coordinates along the left side of Alpena Highway Alignment.....	20
Table 3-3. Resistivity Survey Parameters and Coordinates along the right side of Alpena Highway Alignment.....	20
Table 3-4. Resistivity Survey Parameters and Coordinates along the Landside of the Mel Price Levee.....	25
Table 3-5. Resistivity Survey Parameters and Coordinates along the Riverside of the Mel Price Levee.....	26
Table 4-1. Resistivity soil ranges from the Alpena, AR, Alton, IL sites, and other resistivity tests by Hayashi et al. (2010), Gun et al. (2015), Garman et al. (2004), and Keller & Frischknecht. (1966). ....	42

## **1 Introduction**

Most times, subsurface soil investigations are performed at project sites using traditional geotechnical investigations methods producing subsurface profiles and geotechnical engineering properties of the soil. Traditional geotechnical investigation methods such as Standard Penetration Test (SPT) and Cone Penetration Test (CPT) have proven to be effective, but the process is destructive, slow, expensive, and collects data revealing information at only discrete locations. Capacitively Coupled Resistivity (CCR) a geophysical method could be an improvement on the traditional geotechnical investigation methods because it is nondestructive, rapid, and collects data revealing continuous information of the entire subsurface soil. It could also help focus the drilling and sampling to specific locations identified as critical localized features such as expansive clays, sinkholes, or unknown landfills rather than performing uniform sampling across the site. This thesis explores the applicability of CCR as a subsurface soil investigation method. The CCR testing was conducted at two sites characterized by different soil conditions. The first site was located at Alpena, Arkansas and comprised of clay and silt soil with a deep water table, and the second site was at Alton, Illinois and comprised of clay and sand soil with a shallow water table.

This thesis has five Chapters. Chapter 1 presents the introduction explaining the motivation and organization of the thesis. Chapter 2 presents the literature review explaining the concept of CCR, typical electrical resistivity values established in previous research, the depth of exploration achievable using CCR, and previous research documenting possible applications of electrical resistivity. Chapter 3 presents the methodology and equipment used to conduct CCR testing. Chapter 4 presents the results of the CCR testing and discusses the accuracy, possible application and limitations of CCR. Chapter 5 presents the conclusion and future possibilities achievable using CCR.

## **2 Literature Review**

### **2.1 Introduction**

The purpose of this literature review is to explain the background of Capacitively Coupled Resistivity (CCR) and review literature on its use as a subsurface investigation tool. This chapter will explain the concept of CCR along with the equipment used for data collection, typical electrical resistivity values, and factors that affect the depth of investigation. The final sections will summarize previous research involving electrical resistivity for soil classification and other related areas of research.

### **2.2 Capacitively Coupled Resistivity (CCR)**

The CCR method is a nondestructive near surface geophysical testing method that involves towing equipment shown in Figure 2-1 across the testing site. This literature review will focus on the OhmMapper type of CCR equipment as that is what was used in the research. OhmMapper CCR involves capacitive coupling using a transmitter and receiver with coaxial cables arranged in a dipole-dipole configuration to introduce electric current into the ground as shown in Figure 2-2. The configuration works because the metal shield of the coaxial cable and the soil surface act as two capacitor plates separated by dielectric material between them, which is the outer insulation of the coaxial cable. Alternating current is applied to the coaxial cable side of the transmitter's capacitor causing the generation of alternating current in the soil on the other side of the capacitor. The generated current in the ground moves through the capacitor of the receiver's coaxial cable where the generated voltage is measured from the current flowing through the soil (Allred et al. 2005). The measured voltage is proportional to the resistivity of the soil between the dipoles (Asch, et al, 2008). Due to mobility, the user is able collect high-resolution resistivity data over large areas in a short period.

The apparent resistivity data collected using the OhmMapper is an average of material properties below the surface and does not represent the true layering with depth. To produce true resistivity with depth an inversion process must be completed as with a software package such as RES2DINV (Hickin et al. 2009). RES2DINV performs an inversion on the apparent resistivity data generating an optimized 2D true resistivity model of the subsurface using the least square method (Kuras et al. 2002). The true resistivity values are extracted from the optimized model to create the resistivity subsurface profile as shown in Figure 2-3.



Figure 2-1. The OhmMapper system shown with five receiver dipoles and the transmitter dipole towed by an all-terrain vehicle (Lucius et al. 2008)

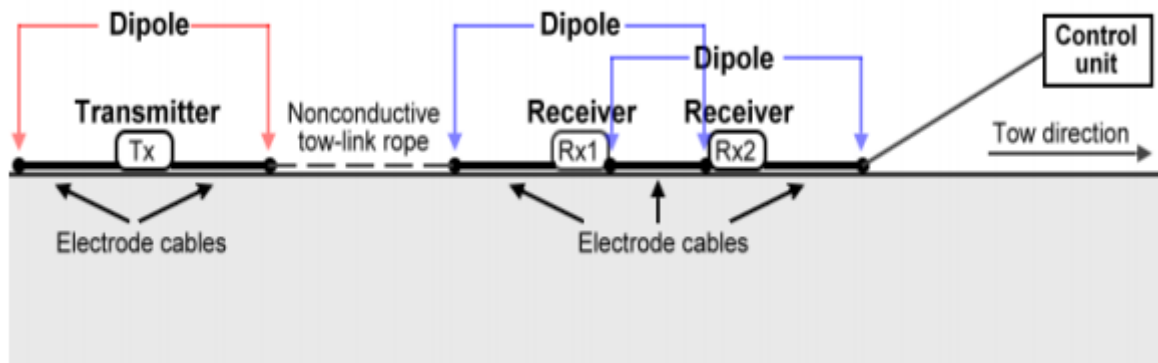


Figure 2-2. A schematic of the OhmMapper capacitively coupled AC resistivity system with one transmitter dipole and two receiver dipoles arranged in dipole-dipole configuration (Lucius et al. 2008)

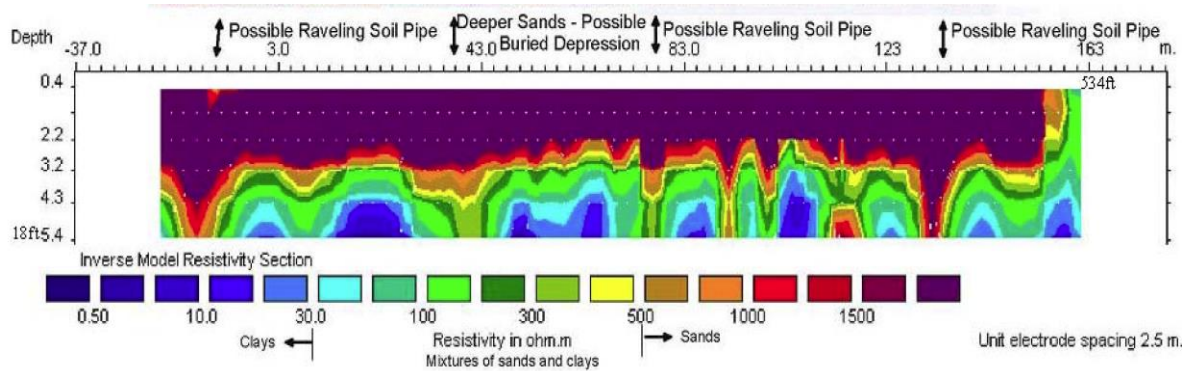


Figure 2-3. Example CCR survey results (Garman and Purcell 2004).

### 2.3 Typical Electrical Resistivity Values for Soil

Early studies concerning the use of resistivity to identify soil types led to the establishment of a range of resistivity values to each major soil type. Palacky (1987), Burger et al. (1992), and Hickin et al. (2009) established resistivity values shown in Table 2-1 using Electromagnetic Resistivity, Electrical Resistivity Tomography (ERT), and CCR surveys respectively.

Table 2-1 has the range of resistivity values for each soil class from each of the above authors. The resistivity ranges differ based on the soil properties, including soil particle structure, arrangement of soil voids, degree of saturation, solute concentration and temperature (Samouelian et al. 2005). In general, the clay or silt soils tend to be the least resistive while the sand and gravel tend to be the most resistive soils. Fine-grained soils (clay or silt) tend to retain higher concentrations of water than coarse-grained soil (sandy or gravelly materials), and since water is very conductive the measured resistivity value is low in fine-grained soils (Lucius et al. 2008). This is because ion exchange property of clay forms a mobile cloud of additional ions around each clay particle, facilitating easy flow of electrical current (Sudha et al. 2009).

Table 2-1. Typical resistivity values established by Palacky. 1987, Burger et al. 1992, and Hickin et al. 2008

Palacky 1987		Burger et al. 1992		Hickin et al. 2008	
Soil Type	Resistivity (ohm-m)	Soil Type	Resistivity (ohm-m)	Soil Type	Resistivity (ohm-m)
clay	2-100	clay or water filled cavities	$\leq 300$	clay, silt and fine sand	$\leq 400$
gravel or sand	500-10000	sand, gravel or bedrock	300-1000	sand	400-800
		bedrock or air filled cavities	$>1000$	gravel	$>800$

## 2.4 Depth of Exploration

For CCR, the depth of exploration has more limitations than conventional resistivity tests like electrical resistivity tomography (ERT) because the system operates at a relatively high frequency (16 kHz). Typically, high frequencies do not penetrate well into good conductors, in this case soil and this tendency is known as the skin depth effect. The target depth of investigation is adjusted by varying the spacing of the transmitter and receiver electrodes (Hickin et al, 2009). Hickin et al. (2009) conducted CCR tests using an OhmMapper setup with five 5m dipole receivers, and a transmitter with a 5 m rope length. The dipole lengths were spaced as shown in Figure 2-4 which produced a vertical pseudo section to a depth of approximately 5 m.

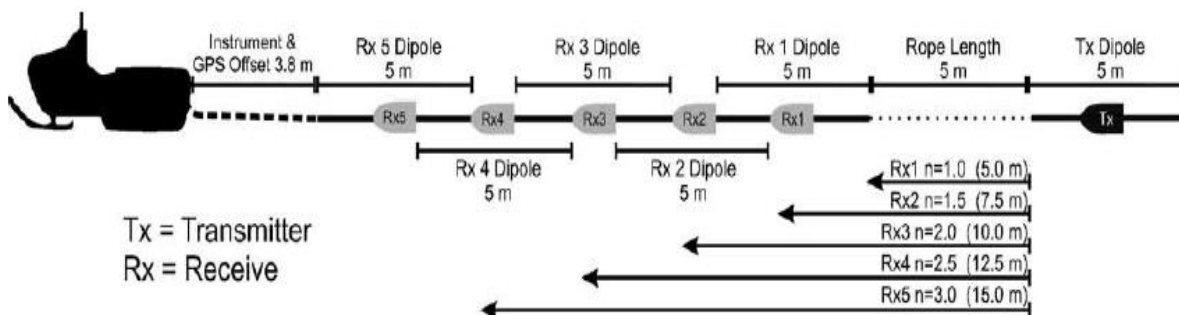


Figure 2-4. OhmMapper configuration with five dipoles and a transmitter (modified from Geometrics 2001) (Hickin et al. 2009)

## 2.5 Previous Research

### 2.5.1 Geophysical Characterization of the American River Levees, Sacramento, California, using Electromagnetics, Capacitively Coupled Resistivity, and DC Resistivity

Asch et al. (2007) conducted a geophysical survey of a portion of American River Levees in Sacramento, California in May 2007 as part of the USGS Survey. Their target was to map the distribution and thickness of sand lenses and determine the depth to a clay unit underneath the sand. The concern was the erosion of the sand lenses could compromise areas along the levee causing levee failure during high water events in highly populated areas of Sacramento. Capacitively Coupled Resistivity (Geometric's OhmMapper) survey and DC Resistivity (Advanced Geosciences, Inc.'s SuperSting R8 systems) survey were used to collect resistivity data and develop soil profiles. Both methods produced consistent inversion results showing potential sand and clay units as shown in Figure 2-5 and Figure 2-6. For the OhmMapper, the dipole spacings used were 5 m and 10 m generating depths of investigation to about 12m. The locations of the sand lenses were closest to the river, while clay deposits were further away from the river. Locations of potential sand deposits are shown in blue colors and the underlying substrate clay units are shown in orange to red colors. These observations when compared with the resistivity color map in Figure 2-6 indicate the clay layer has a resistivity value of at most 300 ohm-m, while the sand and gravel has resistivity value of 600 ohm-m and higher. The results of the geophysical investigation helps U.S. Army Corps of Engineers (USACE) to maintain the levee system and provides an added resource to designers and planners on levee enhancement projects.

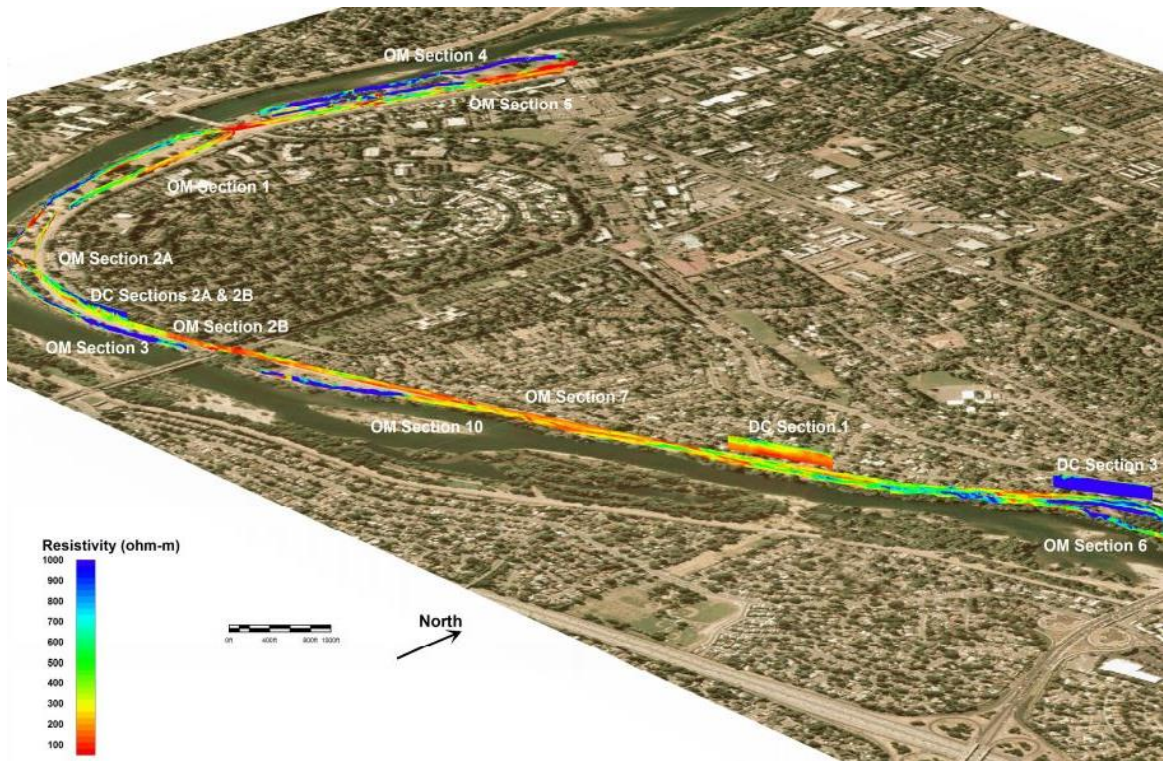


Figure 2-5. USGS American River Levee survey OhmMapper and DC resistivity inversion results in 3D (Asch et al. 2007)

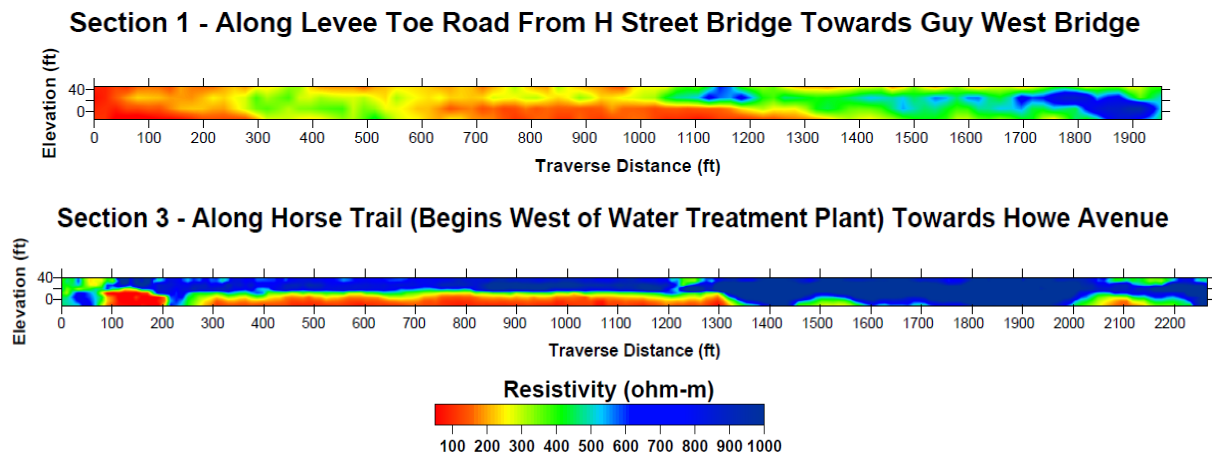


Figure 2-6. Resistivity plots for some sections along the USGS American River Levee survey (Asch et al. 2007)



## 2.5.2 Using Ground-Penetration Radar And Capacitively Coupled Resistivity To Investigate 3-D Fluvial Architecture And Grain-Size Distribution of A Gravel Flood Plain In North East British Columbia, Canada.

This research conducted by Hickin et al. (2009) is significant because it contains information about the use of CCR for architectural analysis of a bar platform and channel bend on the floodplain of a poorly organized wandering gravel-bed river. The subsurface sedimentology of five trenches were observed directly by CCR survey. The CCR survey was conducted with an OhmMapper configured with five, 5 m dipole receivers and a dipole transmitter with a 5 m rope length, arranged in a dipole–dipole array (Geometrics 2001). Positional data was acquired with a hand held GPS and topographic with a high-resolution light detection and ranging survey (LiDAR). The raw apparent resistivity data obtained from the OhmMapper was uploaded into Geometric’s MagMap2000 software where poor data points were removed before individual lines were exported in a format compatible with RES2DINV inversion software. The inversion process was iterative, and parameters were altered systematically until the software generated a model with results reasonably consistent with the field observations. Point data from the 2D inversions performed by RES2DINV were extracted as x,y,z location data with the corresponding true resistivity value and imported into Voxler (Golden Software 2006) to generate a 3D resistivity model. The data was geospatially analyzed by ArcMap.

From their results, resistivity values below 400 ohm-m correspond to fine-grained sediments (clay, silt, and fine sand), values between 400 and 800 ohm-m represent medium-grained sediments (sand), and values greater than 800 ohm-m represent coarse-grained sediments (gravel). Shown in Figure 2-7, most bar and undifferentiated floodplain features have high resistivity values (>800 ohm-m) indicating coarse sediments. The upper 2-3 m of

areas classified as topographic low have resistivity values suggesting sand of fine-grained channel fill shown in Figure 2-7 (Hickin et al, in 2009).

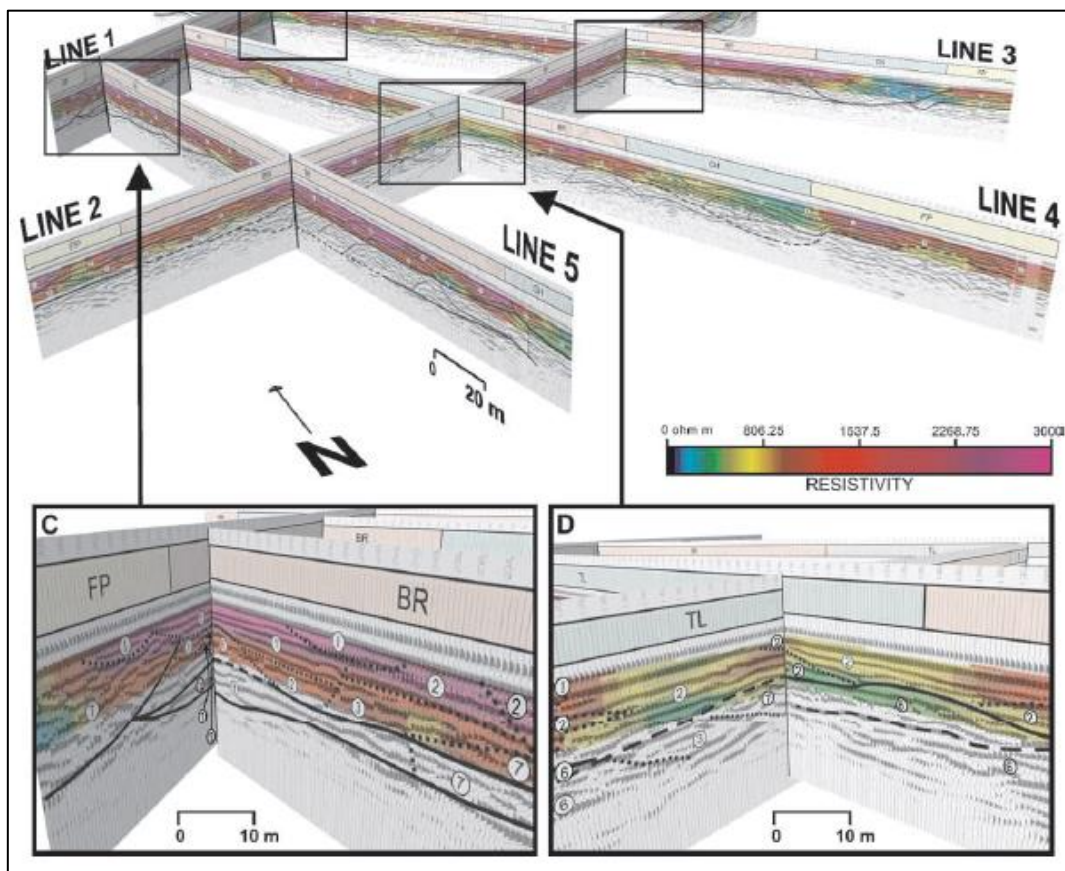


Figure 2-7. Resistivity Plots Along the Lines Traveled By The OhmMapper. (BR is bar, TL is local topographic low, and FP is undifferentiated floodplain).

## 2.6 Other Use of CCR

### 2.6.1 Identify Karst Features

CCR method proved to be a suitable method for determining shallow karst features (Vadillo et al., 2012). To avoid the possibility of disturbance from metal objects to the resistivity results a site with no metal objects such as fences, borehole caps and waste was selected. The OhmMapper system was able to penetrate to a depth of 9 ft. using five receivers with two 5-meter dipole cables for each unit. They expected to find air filled voids from 0.2m to 10 m in width and up to 3m in height. The resistivity plot in Figure 2-8 revealed a high resistivity anomaly in the north west zone with values more than 7500 ohm-m compared to a

background resistivity of 300–1500 ohm-m. It is known that electric-current lines tend to avoid a resistive body such as an air-filled cavity (Vadillo et al, 2012). Since the geology is well known and cavities are the only eligible “anomalous” features in the massive dolostones, we interpret the anomaly as being caused by a cavity (Vadillo et al, 2012).

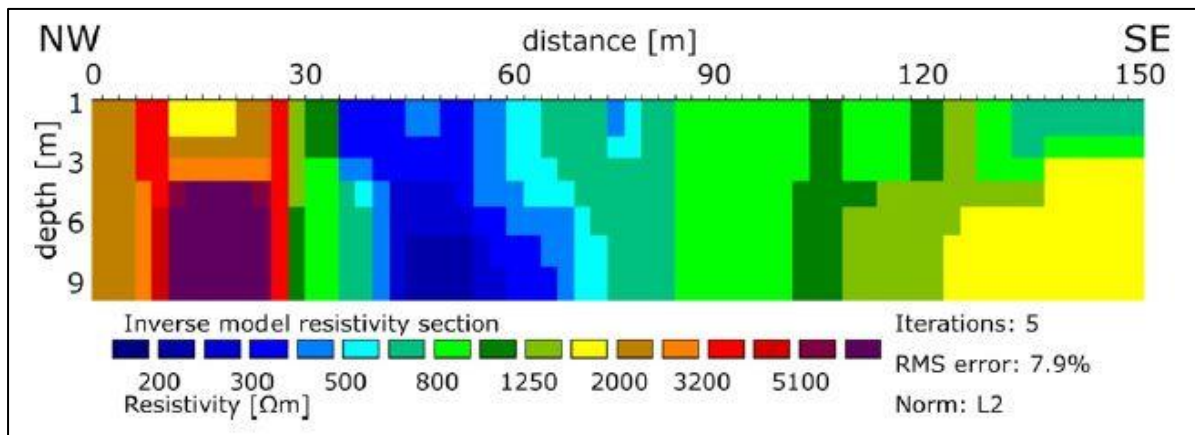


Figure 2-8. Underground resistivity plot based on OhmMapper measurements (Vadillo et al, 2012)

### 3 Methods and Materials

#### 3.1 Introduction

This section presents the methodology and equipment used to conduct Capacitively Coupled Resistivity (CCR) testing at two sites in Alpena, AR, and in Alton, IL shown in Figure 3-1 and at the coordinates shown in Table 3-1. The procedures to test the validity of this method as a subsurface soil characterization tool are also presented. In this section, the Alpena, AR, and Alton, IL sites are referred to as Alpena Highway Alignment and Mel Price Levee. The Alpena site is the location of a highway expansion project changing US 62 from a two lane to four lane highway, and the Alton site is a levee along a portion of the Mississippi River.

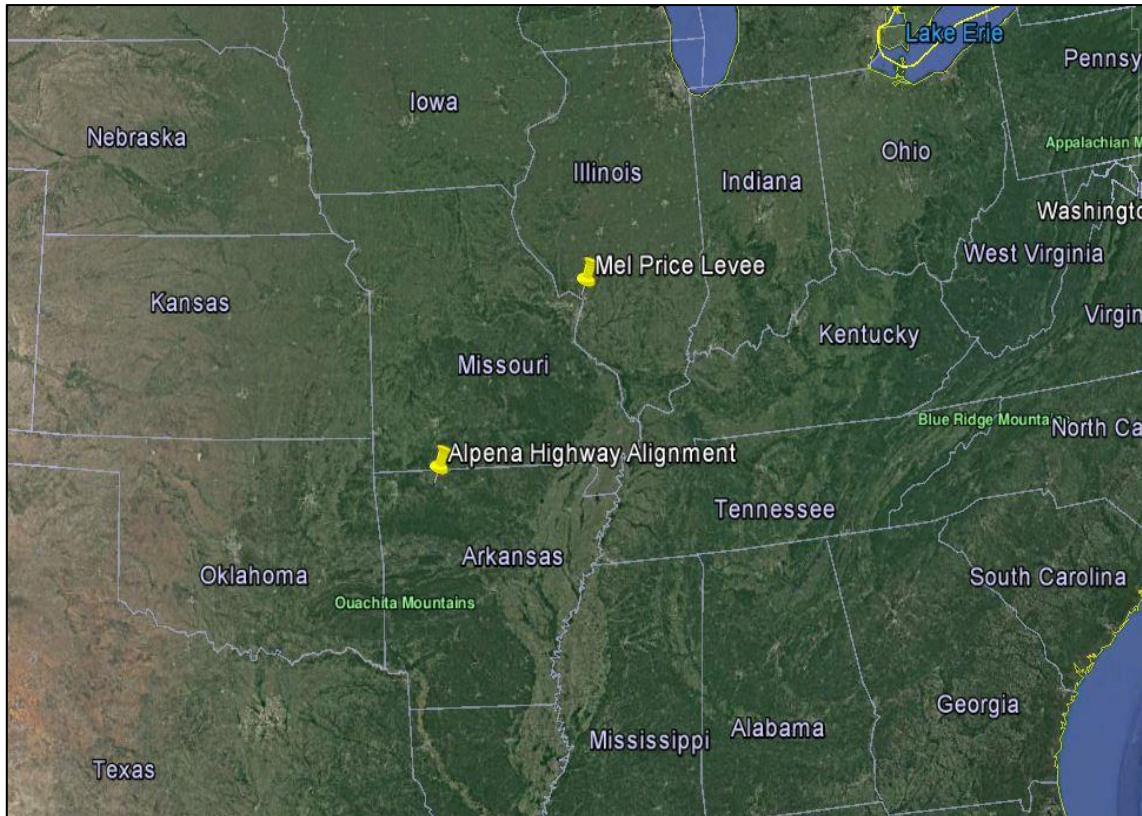


Figure 3-1. Resistivity Analysis Location at Mel Price Levee and Alpena Highway Alignment

Table 3-1 Coordinates showing the location of Capacitively Coupled Resistivity Test sites

Site	Center Point Location
Alpena Highway Alignment	36.302658°, -93.350932°
Mel Price Levee	38.876190°, -90.169328°

### 3.2 Capacitively Coupled Resistivity

Capacitively coupled resistivity (CCR) is a method used to determine the resistivity of soil with depth. It consists of a dipole-to-dipole configuration between a transmitter and receiver. The transmitter and receivers are placed on the ground surface as shown in Figure 3-2 and create a capacitance between the conductor (dipole cables) and the ground allowing the AC current to flow from the transmitter through the ground where the receiver measures it. This method allows the collection of resistivity data at a rapid rate compared to other

methods that measure electrical resistivity. More details on the principles of CCR testing are provided in Chapter 2. The following sections present details of the testing sites, equipment, data acquisition and data processing techniques used to conduct the CCR test at the two sites.

### 3.2.1 General Data Acquisition Methodology

The equipment used to collect the apparent (raw) resistivity data using the CCR method was the Geometrics TR5 OhmMapper system. It consists of a transmitter, five receivers, dipole cables, non-conductive rope, laptop (data logger), and Trimble Geo 7x GPS unit as shown in Figure 3-2. The system is connected in series (a long line) and towed along the ground surface by an all-terrain vehicle (ATV) as shown in Figure 3-2.



Figure 3-2. A) Transmitter and Receivers B) Dipole Cables connected to receivers with protective shields at the site. C) Data logger with Trimble Geo 7x GPS device mounted on the All-Terrain Vehicle (ATV) D) OhmMapper setup towed in a line by ATV along US 62 near Alpena, Arkansas.

Shields placed over the transmitter and the receivers during towing, as shown in Figure 3-2, protect the units from wear and tear. The transmitter and receivers are powered by two 6V DC batteries. Dipole cables are used to connect the receivers with a single dipole cable connected to each end of the receivers and transmitter. A rope attached at one end to the transmitter's dipole cable and at the other end to the first receiver's dipole cable allows the

transmitter to be towed at a constant distance from the receivers. The transmitter sends an alternating current into the ground, which is picked-up and measured by the receivers at a voltage accuracy of 1%. Dipole cables connect the five receivers to each other with each recording resistivity data at different distances away from the transmitter (i.e., different apparent depths of investigation). The Trimble Geo 7x device acquires high quality GPS data at an accuracy of 1 to 2 meters. The data logger (laptop) mounted on the ATV records the resistivity readings and GPS data as the OhmMapper passed over the ground surface.

The depth of investigation of the OhmMapper is dependent on the dipole length, the rope length, and the ground resistivity of the site. At highly resistive sites, the separation between the transmitter and receiver can be much longer than would be possible at less resistive sites since the transmitter signal can be reliably detected and decoded at longer distances or deeper depths. A general rule of thumb is the maximum depth of investigation will be about one-fifth ( $1/5$ ) of the total array length (Geometrics 2007).

### 3.2.2 Data Processing

The computer software used to process the acquired resistivity data and produce the 2D resistivity profiles are, OhmImager, MagMap, Res2Dinv and surfer. This section presents background information on each of the software used and the steps taken to generate the resistivity profiles. OhmImager is used to read the raw resistivity data acquired from the various OhmMapper setups (rope length, dipole length, operator offset) along the same line, correct potential setup metadata errors, and generate a model suitable for exporting the data to MagMap. MagMap is used to filter the data for noise and convert the filtered data into a format suitable for the inversion process. Res2Dinv is used to perform an inversion converting the raw data to true resistivity values. Surfer is used to plot the true resistivity values as a 2D cross section plot.

The OhmImager software, developed by Geometrics, is used to inspect the apparent resistivity data measured in the field. The first step is to ensure the acquisition parameters saved in the raw data file matches the parameters used in the field. By reading in the raw resistivity data, OhmImager generates a model as shown in Figure 3-3 displaying apparent resistivity vs distance along the OhmMapper travel path and converts the GPS data (latitude and longitude) acquired by the Trimble Geo 7x device to linear distance along a line. For the final step, OhmImager exports the apparent resistivity model into a format accessible by MagMap for the next processing phase. In situations where multiple setups are used (i.e., various rope lengths or dipole lengths), the individual data files can be combined into one exportable data set for further processing using MagMap.

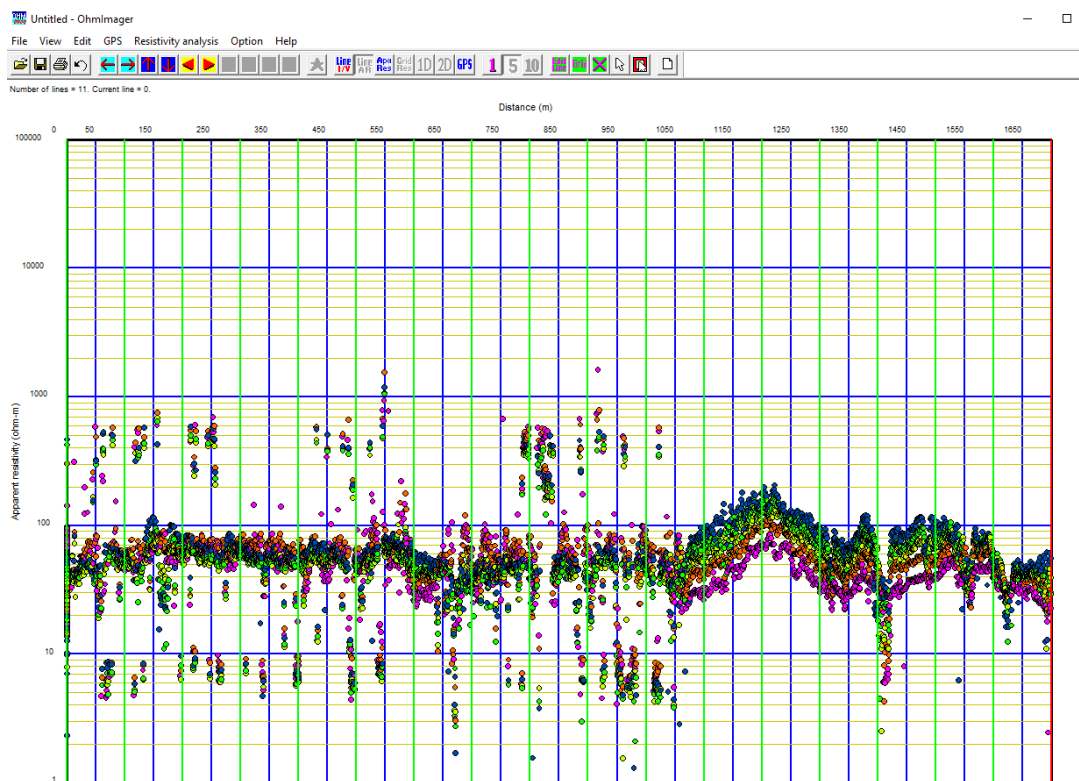


Figure 3-3. OhmImager Screen showing the apparent resistivity vs distance plot modeled from data acquired by the OhmMapper.

The Geometrics software MagMap is used to filter out the noise from the measured resistivity data by removing spikes and dropouts as shown in Figure 3-4. It also displays the path traveled by the OhmMapper capturing points along the



alignment since it is not a straight line. MagMap completes the preparation of the data for the inversion process by creating a resistivity pseudo section with soil depth vs distance as shown in Figure 3-5 along the OhmMapper travel path and exports the filtered data to a format accessible by the Res2DInv software. To complete the export process, the user selects an electrode spacing for data averaging which affects the degree to which changes in resistivity between soil layers can be visualized in the final plot.

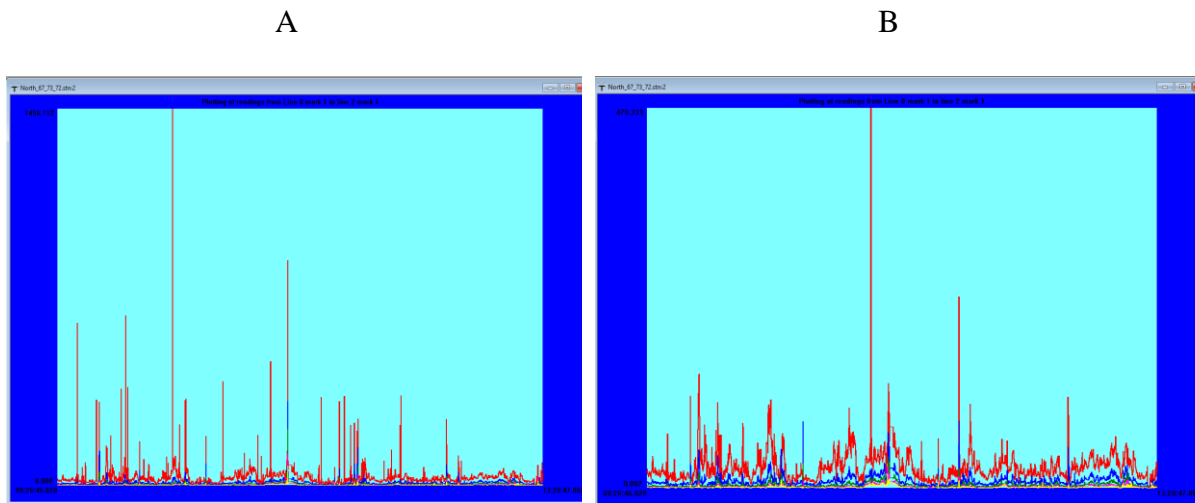


Figure 3-4. MagMap Screenshot showing A) before and B) after the resistivity data filter process for spikes and dropouts.

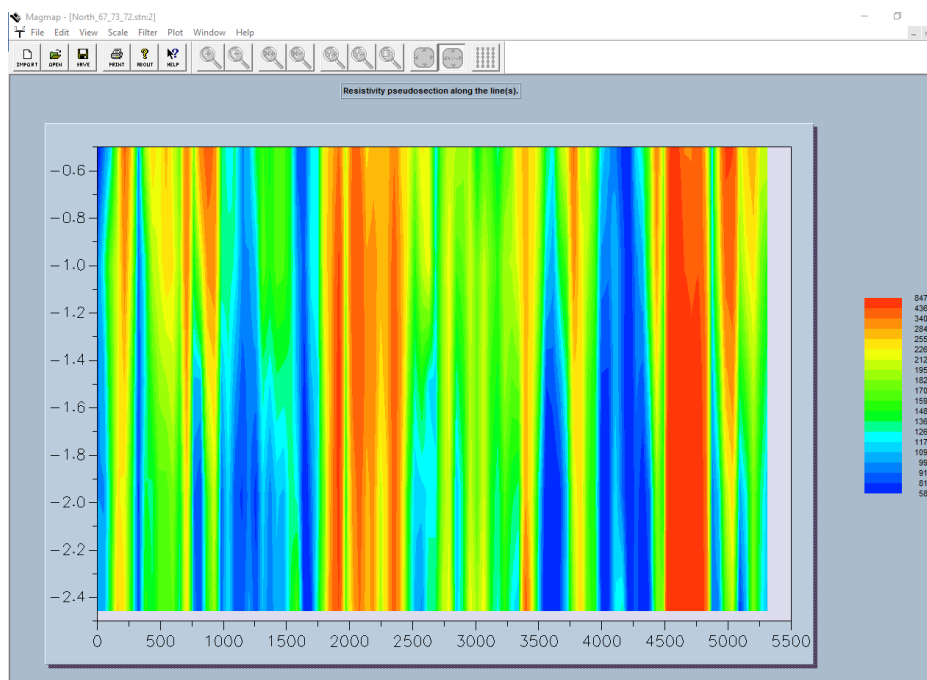


Figure 3-5. MagMap Screenshot showing resistivity pseudosection along the travel path.

Res2DInv, a windows based software developed by Geotomo Software, is used to develop a 2D resistivity model for the subsurface from data obtained from electrical imaging surveys (Dahlin 1996; Loke et al. 2003). Apparent resistivity values are calculated using finite element modelling, and a non-linear smoothness-constrained least-squares optimization technique (deGroot-Hedlin and Constable 1990; Loke et al. 2003). Res2DInv carries out an inversion on the measured data converting the apparent resistivity values to the true resistivity values. The inversion algorithm minimizing the absolute values of differences between observed and calculated data in an iterative manner. The inversion of the field data is carried out until a point when the absolute error value (abs) ceases to reduce. The result is a data file containing coordinates, distance, elevation, and resistivity values along the path traveled by the OhmMapper. To create the resistivity plot Res2DInv exports the created data file to a format accessible by surfer.

Surfer is a software developed by Golden software for generating maps quickly and easily. Surfer performs a triangulation with linear interpolation gridding method on the data. This generates a grid by combining various depths of data to create a single profile showing resistivity as a function of depth and distance as shown in Figure 3-6. The soil resistivity ranges for the created profiles are adjusted using surfer to fit the typical values or match the soil boring records for the site. The adjustment is performed by manually changing the color map ranges in order to better separate the geotechnical materials based on information from the boring logs. The representative profile is selected from the adjusted soil profiles as the one that best predicts the subsurface condition at the site based on distance covered, depth of exploration and similarity to existing soil boring records.

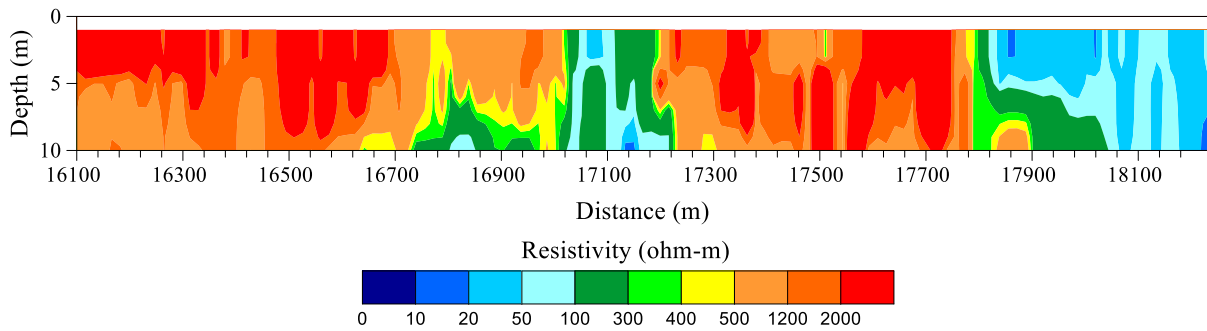


Figure 3-6. Sample resistivity profile generated by Surfer.

### 3.3 Alpena Testing

The Alpena site is a 19,200 feet portion along the right and left side of the US 62 highway located about 6000 feet west of the city of Alpena Arkansas with predominantly dry ground conditions at the time of testing. CCR testing took place on the 2<sup>nd</sup> day of November in 2017 along the right and left side of the road starting and ending at the coordinates shown in Table 3-2 and Table 3-3. The precipitation records from the closest National Centers for Environmental Information National Oceanic and Atmospheric Administration (NOAA) station to the testing site in Springfield Missouri for the month of October 2017 leading up to the CCR testing date shown in Figure 3-7 indicates 2.47 inches of precipitation. The preexisting borings were drilled along both sides of the road as shown in Figure 3-8 and spaced 800 to 1000 feet apart at a distance ranging from 4 to 32 feet away from the road. The Arkansas State Highway Transportation Department (AHTD) materials division on the 23<sup>rd</sup> day of September 2013 conducted the sampling and testing of the soil samples collected from the boring logs shown in Figure 3-9. The soil samples were classified using the American Association of State Highway and Transportation Officials (AASHTO) soil classification method. The boring logs provide soil properties such as the Liquid Limit (LL), Plastic Index (PI) and Moisture Content (% Moisture) of the soil important for soil classification, as well as the soil classifications. The soil classifications present at the site are A-4, A-6, and A-7-6, which are silty and clayey soils. Most borings were to a depth of 5 feet, with a few shallow locations where the auger hit refusal prior to reaching 5 ft (areas believed to be bedrock or

similar material). None of the boring logs show the water table level which is likely an indication of dry conditions and a deep water table at the site. The precipitation records from the NOAA station in Springfield Missouri for the month of August 2013 leading up to the AHTD testing date shown in Figure 3-7 indicates 5.85 inches of precipitation. The precipitation records from the period the samples were tested to the period the CCR survey was conducted reveal a reduction in precipitation from 5.85 inches to 2.47 inches. Such a difference in precipitation could result in the moisture content of the subsurface soil being less on the day the CCR testing was conducted than when the testing of the samples was conducted which could potentially result in poor correlations between soil properties and resistivity. This site is significant for subsurface soil classification using CCR because the dry conditions would reveal the nature of this method in such conditions, and the presence of clay, silt and potential bedrock present a situation where soil differentiation is possible. The test would reveal the accuracy of CCR to characterize subsurface soil and detect possible irregularities along the highway alignment that could be hazardous to design and maintenance.

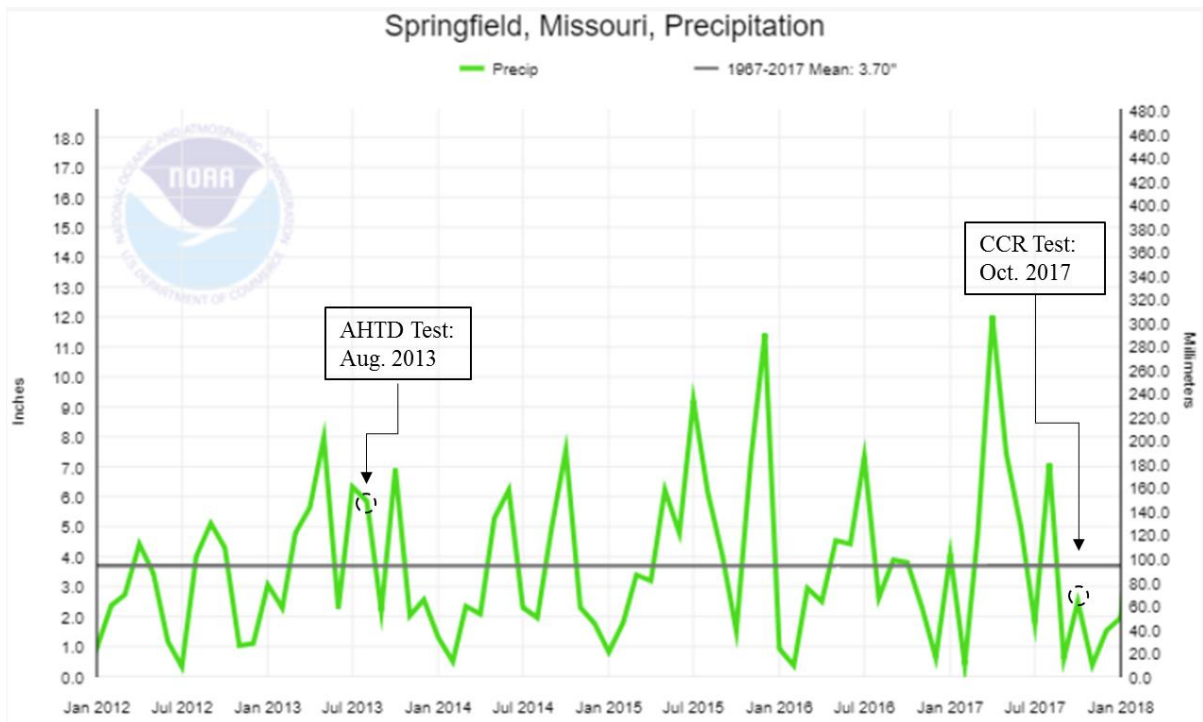


Figure 3-7. NOAA Station in Springfield Missouri precipitation records from January 2012 to January 2018.

Table 3-2. Resistivity Survey Parameters and Coordinates along the left side of Alpena Highway Alignment

Rope Length	Dipole Length	Start	End
m	m	Latitude, Longitude	Latitude, Longitude
2.5	5	36.317798°, -93.374410°	36.296893°, -93.319724°

Table 3-3. Resistivity Survey Parameters and Coordinates along the right side of Alpena Highway Alignment

Rope Length	Dipole Length	Start	End
m	m	Latitude, Longitude	Latitude, Longitude
2.5	5	36.317474°, -93.374431°	36.296718°, -93.319297°

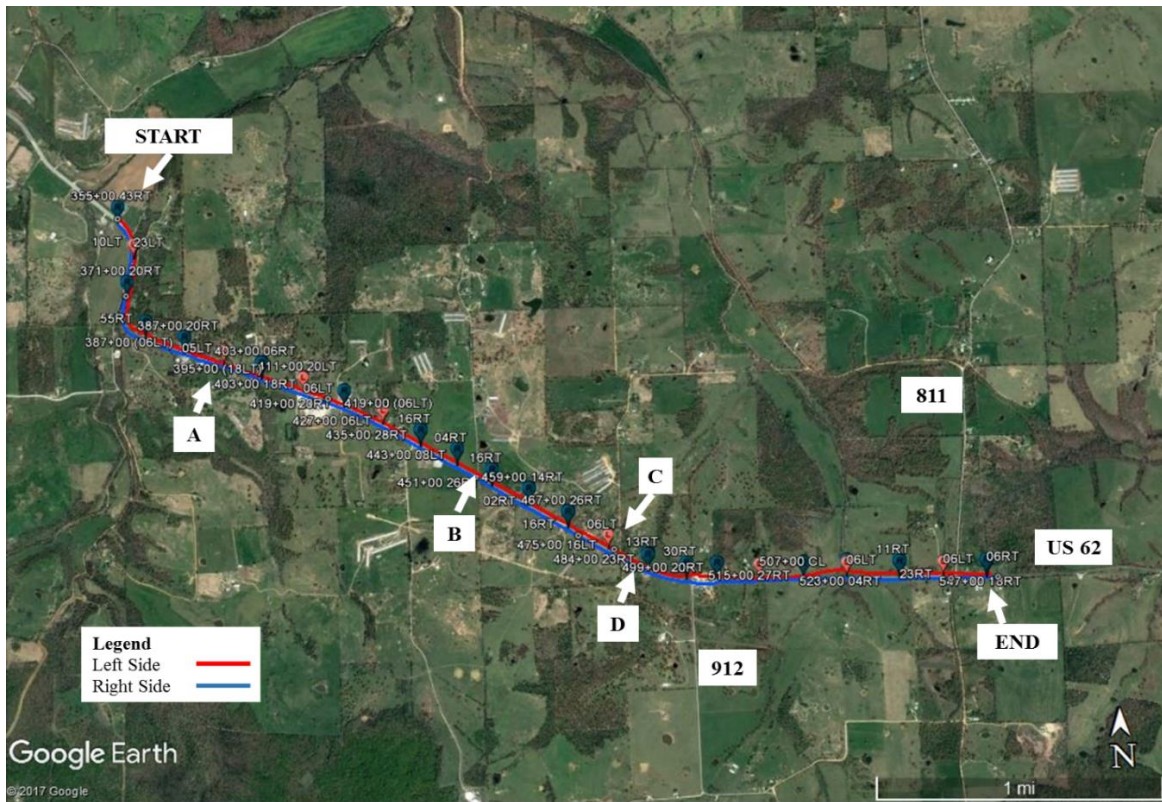


Figure 3-8. Alpena Highway Alignment showing the start and end positions of the data acquisition process along both sides of the highway conducted using the OhmMapper. Letters in the figure correspond to pictures in Figure 3-10.

<b>JOB: 090230</b>				<b>Arkansas State Highway Transportation Department</b>									
<b>JOB NAME: CO.RD 914 - WEST (S)</b>				<b>Materials Division</b>									
<b>COUNTY NO. 8 DATE TESTED 9/23/2013</b>				<b>Michael Benson, Materials Engineer</b>									
<b>STA.#</b>	<b>LOC.</b>	<b>DEPTH</b>	<b>COLOR</b>	<b>#4</b>	<b>#10</b>	<b>#40</b>	<b>#80</b>	<b>#200</b>	<b>L.L.</b>	<b>P.I.</b>	<b>SOIL CLASS</b>	<b>LAB #:</b>	<b>%MOISTURE</b>
				<b>S</b>	<b>I</b>	<b>E</b>	<b>V</b>	<b>E</b>					
363+00	23lt	0-5	BROWN	95	91	88	85	80	56	37	A-7-6(31)	RV1861	
419+00	20rt	0-5	BROWN	98	93	91	88	82	21	09	A-4(2)	RV1862	
539+00	19lt	0-5	BROWN	77	65	60	57	50	41	25	A-7-6(10)	RV1863	
355+00	20rt	0-5	BROWN	90	77	65	60	49	31	15	A-6(4)	S1813	18.7
355+00	32rt	0-5	BROWN	93	87	77	70	63	40	20	A-6(11)	S1814	23.2
355+00	43rt	0-5	BROWN	95	88	76	73	62	36	19	A-6(9)	S1815	23.5
363+00	10lt	0-5	BROWN	95	89	81	76	67	40	23	A-6(12)	S1816	17.3
363+00	23lt	0-5	BROWN	95	88	80	75	65	34	19	A-6(8)	S1817	22.9
363+00	39lt	0-5	BROWN	100	92	82	77	69	58	32	A-7-6(32)	S1818	45.7
371+00	20rt	0-5	BROWN	95	88	81	76	72	31	16	A-6(9)	S1819	25.3
387+00	06rt	0-5	BROWN	96	93	87	85	82	22	04	A-4(0)	S1821	18.1
387+00	20rt	0-5	BROWN	100	92	82	77	69	38	23	A-6(21)	S1822	14.1
395+00	05lt	0-5	BROWN	96	95	90	86	82	ND	NP	A-4(0)	S1823	8.1
395+00	18lt	0-3.5z	BROWN	94	88	88	83	72	ND	NP	A-4(0)	S1824	4
403+00	06rt	0-5	BROWN	98	95	92	90	77	17	03	A-4(0)	S1825	15.5
403+00	18rt	0-5	BROWN	97	95	95	95	78	21	05	A-4(1)	S1826	15.1
411+00	06lt	0-5	BROWN	98	94	91	87	70	23	08	A-4(3)	S1827	14.8
411+00	20lt	0-5	BROWN	90	87	83	78	62	24	06	A-4(1)	S1828	12.4
419+00	06rt	0-5	BROWN	98	95	91	85	65	24	11	A-6(4)	S1829	15.5
419+00	20rt	0-5	BROWN	100	98	95	88	67	29	16	A-6(8)	S1830	17
427+00	06lt	0-5	BROWN	96	92	88	80	72	28	11	A-6(6)	S1831	19
427+00	19lt	0-5	BROWN	99	99	97	91	73	32	19	A-6(11)	S1832	18.1
435+00	16rt	0-5	BROWN	97	93	88	84	70	ND	NP	A-4(0)	S1833	15.4
435	28rt	0-5	BROWN	95	91	88	86	73	ND	NP	A-4(0)	S1834	14.9
443+00	04rt	0-5	BROWN	97	92	88	88	66	ND	NP	A-4(0)	S1835	16.8
443+00	08lt	0-5	BROWN	98	95	90	81	78	22	03	A-4(0)	S1836	11.9

**comments:** LOCS. MEASURED FROM CL CONST. Z=AUGER REFUSAL, W=MULTIPLE LAYER  
X=STRIPPED

Friday, September 27, 2013  
Page 1 of 2

Figure 3-9. AHTD Job 090230 soil boring log for a portion along US 62 highway west of Alpena, AR

During data acquisition, the OhmMapper was towed about 5-20 feet away from the highway as shown in Figure 3-10. This was due to safety concerns presented by traffic along the highway, and the need to be reasonably close to the borehole locations. The equipment had to travel over the highway pavement at locations where the shoulder narrowed or had little or no natural shoulder. A rope length of 2.5 meters connected the transmitter to the five receivers with dipole lengths of 5 meters. This setup produced a resistivity profile 6 meters

deep at the Alpena site. The CCR data acquired at the Alpena site was processed according to Section 3.2.2.

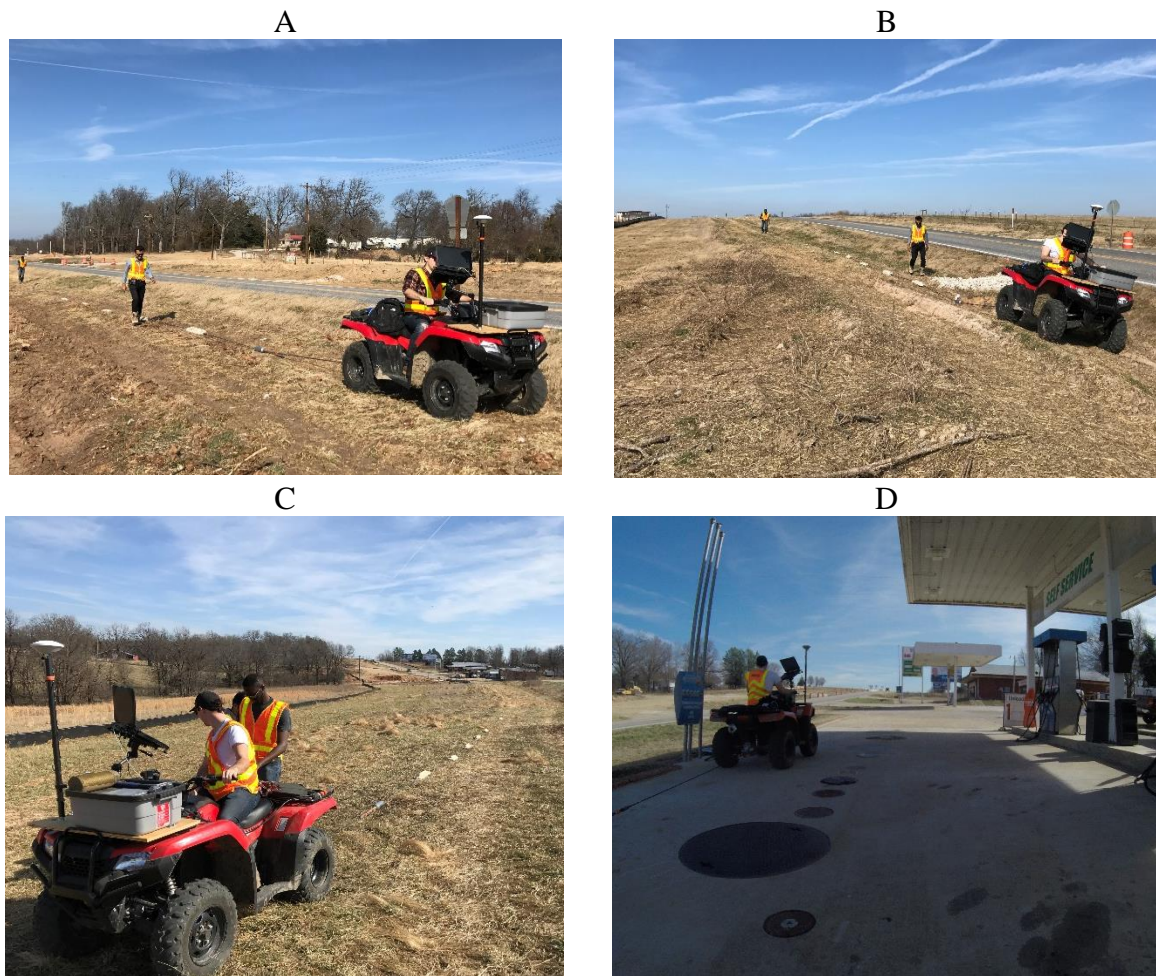


Figure 3-10. Along the Alpena Highway alignment OhmMapper towed at; A) STA 403+00 right side of highway, B) STA 451+00 passing over a buried utility crossing the highway on the right side, C) STA 484+00 left side of the highway, D) STA 491+00 passing through a gas station on the right side of the highway.

#### 3.4 Mel Price Levee Testing

The Mel Price Levee site is a 14,500 foot long section of the Mel Price Levee, which is a 33 foot tall earthen levee located along the Mississippi river as shown in Figure 3-11. The soil conditions were wet illustrated by Figure 3-12 showing visible surface water at portions of the landside of the levee, evidence of a very shallow water table was also observed in P-wave refraction data collected at the site, but not discussed here (Rahimi et al. 2018). Testing took place along the landside and riverside of the levee starting and ending at the coordinates



shown in Table 3-4 and Table 3-5. The levee had boring log data on the landside with example log shown in Figure 3-13, and CPT log data on the riverside example log shown in Figure 3-14. The landside has 85 boring logs from borings spaced approximately 30 feet apart, and the riverside has 25 CPT logs spaced approximately 300 feet apart. The borings were done to depths of over a 100 feet, while most of the CPT data were shallower to depths of 10 feet, with a few like the one shown in Figure 3-14 going to a depth of 30 feet. The boring logs revealed the presence of Fat Clay (CH) and Lean Clay (CL) at the top 6 feet, Silty Sand (SM) 1 meter below the clay layer, and Poorly Graded Sand (SP) below the Silty Sand layer. The boring log also provides the Liquid Limit (LL), Plastic Index (PI) and the size of the sieve through which only 10% of the soil grains pass (D10). The CPT log revealed a top 8 feet of clayey sand and the remaining profile a very thin clay layer of 4 feet sandwiched by two sand layers above and below. A site such as this with clearly defined layers of near surface clay and sand deposits presents ideal characteristics for determining the optimum setup of transmitter and dipole lengths to predict soil stratigraphy accurately in similar sites.



Figure 3-11. Mel Price Levee showing the start and end positions of the data acquisition process along the landside and riverside of the levee conducted using the OhmMapper.



Figure 3-12. A) Visible surface water at landside of Mel Price Levee at sta. 123+00, B) View from top of road showing the pond along the landside of the Mel Price Levee at sta 95+00, and C) OhmMapper towed along riverside of Mel Price Levee at sta 82+00.

Table 3-4. Resistivity Survey Parameters and Coordinates along the Landside of the Mel Price Levee

Rope Length	Dipole Length	Start	End	Depth of Investigation
m	m	Latitude, Longitude	Latitude, Longitude	m
2.5	5	38.876924°, -90.157079°	38.871062°, -90.147422°	5
5	10	38.877102°, -90.157312°	38.871267°, -90.147941°	13
20	10	38.876719°, -90.156867°	38.871074°, -90.147500°	13
30	10	38.877123°, -90.157320°	38.871370°, -90.148188°	17

Table 3-5. Resistivity Survey Parameters and Coordinates along the Riverside of the Mel Price Levee

Rope Length	Dipole Length	Start	End
m	m	Latitude, Longitude	Latitude, Longitude
5	10	38.883179°, -90.169747°	38.867314°, -90.140463°
20	10	38.882730°, -90.169242°	38.875630°, -90.157333°
40	10	38.883169°, -90.169720°	38.876137°, -90.157919°

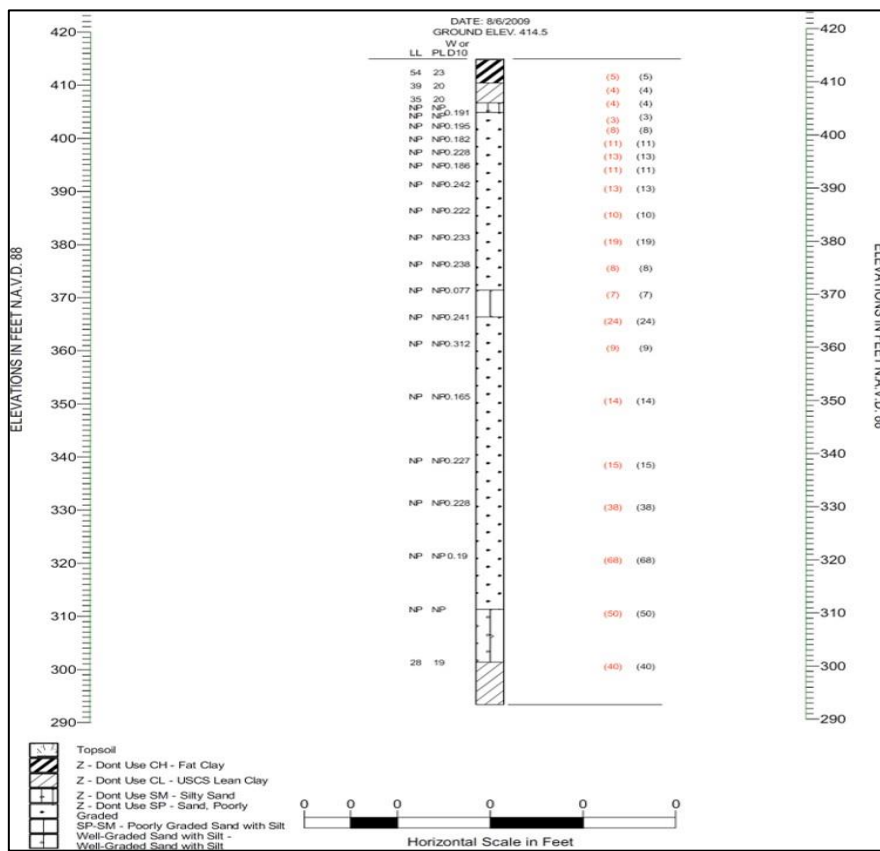


Figure 3-13. Soil boring log collected along the landside toe of the Mel Price Levee.

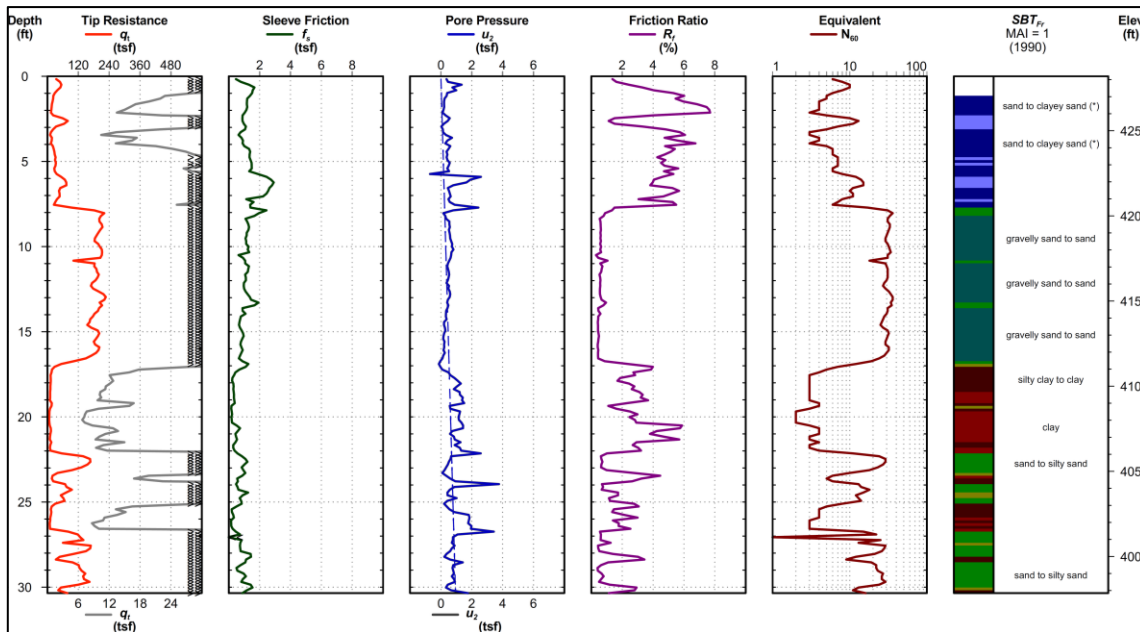


Figure 3-14. CPT log collected along the riverside toe of the Mel Price Levee.

The toe is described either side of the levee as the landside and the riverside which is closer to the Mississippi river. The OhmMapper shown in Figure 3-15 acquired data at each part of the levee using multiple rope length and dipole length setups shown in Table 3-4 to generate resistivity profiles. Performing acquisition at multiple setups helped increase the quality of resistivity data at the deeper depths of investigation.

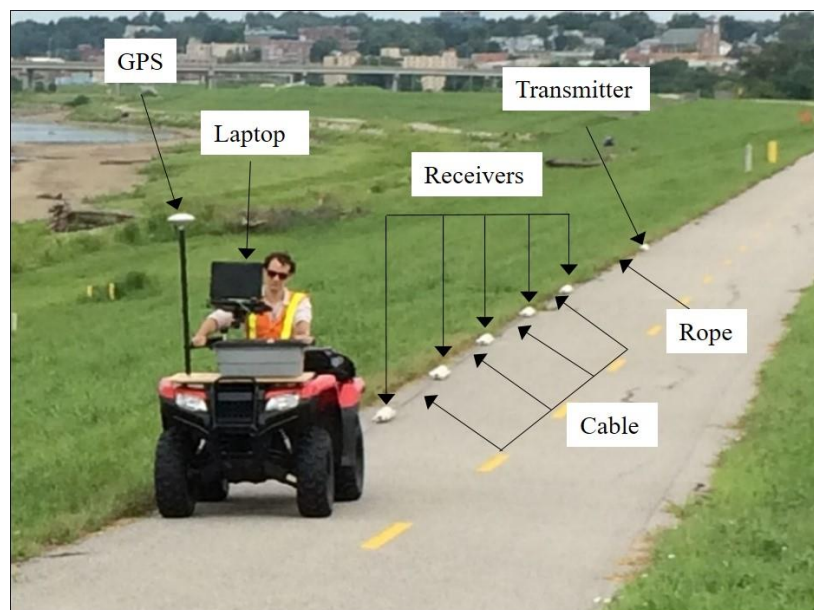


Figure 3-15. OhmMapper towed along the top of the Mel Price Levee collecting resistivity data.

The processing of the CCR data acquired along the levee took place according to Section 3.2.2. For the inversion process, the data was averaged at an electrode spacing of 1.25 meters to aid with identifying the presence of a possible thin silt layer between the clay layer and sand layer. The inversion process performed in Res2Dinv created the 2D inversion model of the subsurface as shown in Figure 3-16 to depths of investigation listed in Table 3-4. All the inversion models created are compared to the boring and CPT logs to select the most accurate depiction of the subsurface profile.

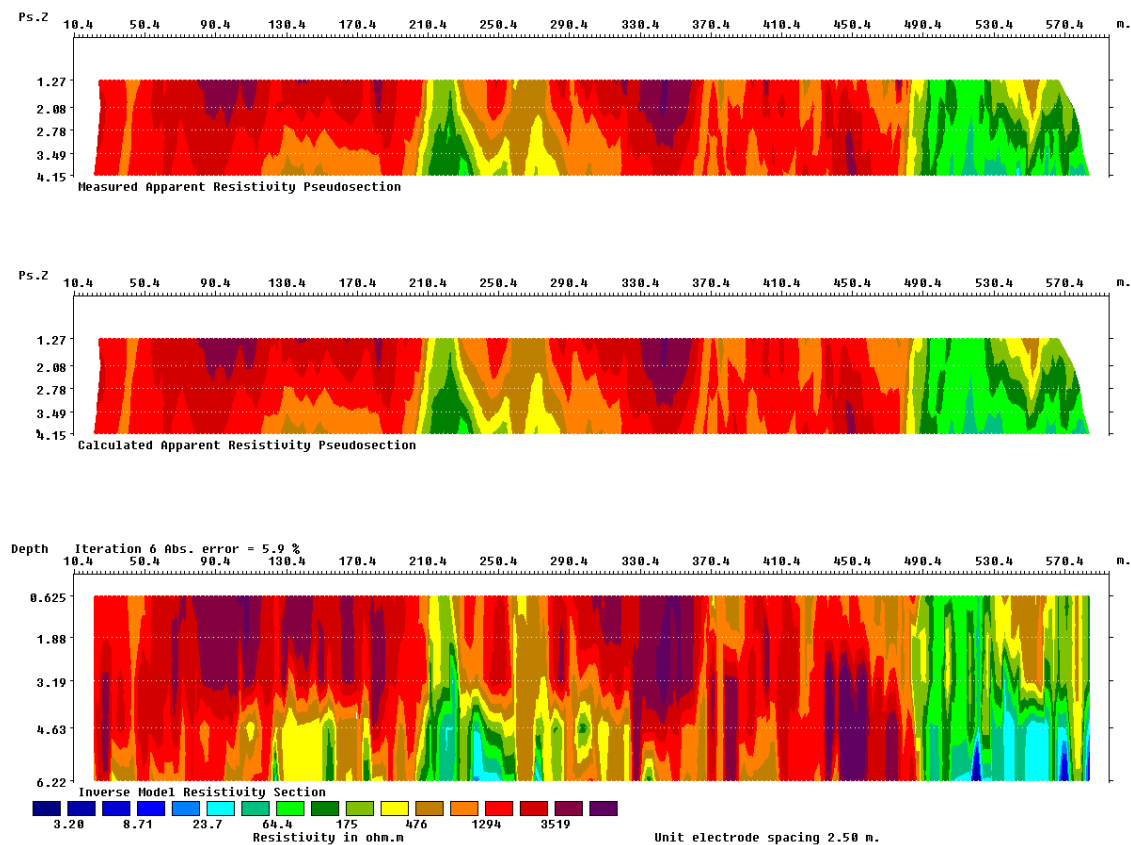


Figure 3-16. Sample subsurface 2D inversion model generated by RES2DINV software.

## 4 Results

### 4.1 Alpena

The resistivity profiles generated from the data acquisition and processing at the Alpena site are shown in Figure 4-1. The cross symbols represent the maximum drilling and sampling depth of each borehole. Above each cross symbol is the soil type identified in the AHTD boring log (presented in Chapter 3) and the station along the highway. Potential areas of significance along the project site are low resistivity clay segments, and potential bedrock segments. The maximum borehole depth of investigation is 5 feet (1.5 meters) from the surface. The resistivity plots presented in Figure 4-1 reach a depth of 6 meters below the surface. The color map below the profile was created using the typical resistivity values (presented in chapter 2) as a basis, then the resistivity ranges are changed till the resistivity profile best represents the boring log data for the site. The profile shows reoccurring layers of clay and silts with a few locations having potential bedrock.

The resistivity soil profiles for the left and right side of the road shown in Figure 4-1, display measured soil resistivity values that identified the same soils as the borings logs between Stations 363+00 and 539+00 on the left side of the road, and Stations 355+00 and 547+00 on the right side of the road. The exception occurs at Station 531+00 on the right side of the road where the predicted clay sample appears as a more resistive material within a soil section of predominantly clay soils between Stations 484+00 to 547+00. However, the soil sample was taken at a location close to an isolated portion of high resistivity soils. Such a scenario with clay and rock in close proximity changes the resistivity value (by averaging multiple material properties together) during the data averaging process leading to the conflict between the resistivity results and the soil sampling results. Stations 523+00 and 539+00 have resistivity values ranging from 300-450 ohm-m, which falls on the soil resistivity boundary of clay or silt and sand or bedrock material observed along the Alpena

site. The samples at Station 523+00 and 539+00 appear to also have been collected at a location where a layer of low and high resistivity soil appear in close proximity subjecting the low resistivity soil to increases in resistivity similar to the scenario discussed for Station 531+00. The three locations where the boring logs indicated potential bedrock all occur along the left side of the road at Stations 395+00, 499+00 and 507+00. From the three locations, the resistivity profile and boring logs agree at only Station 395+00 where the resistivity range is 500-900 ohm-m indicating bedrock. At Station 499+00 the estimated resistivity at the location ranges from 200-300 ohm-m falling on the boundary between clay or silt and sand or bedrock material indicating it has an equal chance of being either material. At Station 507+00 the estimated resistivity is within the range of 50-150 ohm-m indicating clay or silt rather than bedrock.

The relationship between soil properties and resistivity along with the error deviation of each soil sample is displayed using error bars as shown in Figure 4-2, Figure 4-3 and Figure 4-4, for moisture content, plastic index, and liquid limit, respectively. The soil samples in the figures were classified as clay, silt and sand based on the AASHTO soil classification system. Soils classify as granular materials if 35% or less of the soil sample passes the No. 200 sieve and silt-clay materials if more than 35% passes the No. 200 sieve. The silt samples have symbols A-4 identifiable when LL is 40 max and PI is 10 max, and A-5 identifiable when LL is 41 min and PI is 10 max. The clay samples have symbols A-6 identifiable when LL is 40 max and PI is 11 min, A-7-5 identifiable when LL is 40 max and PI is 11 min ( $PI \leq LL-30$ ), and A-7-6 identifiable when LL is 41 min and PI is 11 min ( $PI > LL-30$ ). Therefore, the PI and LL are the primary separators between clay and silt soils in the AASHTO classification system.

The error bars show the extent to which the resistivity of each soil sample deviates from the resistivity value of 150 ohm-m selected in an attempt to hypothetically separate the

clay samples from silt samples based on the resistivity data measured at the Alpena site. The soil samples with resistivity less than 150 ohm-m are hypothetically classified as clay samples, while those with resistivity greater than 150 ohm-m are hypothetically classified as silt samples. The error bar is displayed for samples identified as clay in the boring logs with resistivity values greater than 150 ohm-m, and silt in the boring logs with resistivity values less than 150 ohm-m.

Figure 4-2 shows the relationship between moisture content (MC) and resistivity along with the error distribution for the Alpena data. The soil samples can be separated using moisture content evident by a majority of clay samples having MC greater than 15% while the majority of silt samples have a MC less than 15%. Figure 4-3 shows the relationship between plastic index (PI) and resistivity for the Alpena data. Most clay samples have a PI greater than 10 while most silt samples have a PI less than 10 matching the AASHTO soil classification criteria for both soil types as expected highlighting the role played by PI in identifying and classifying both soils using the AASHTO system. Figure 4-4 shows the relationship between liquid limit (LL) and resistivity for the Alpena data. Most clay samples have a LL between 22 and 42 indicating mostly A-6 and a few A-7-6 samples, and most silt samples have LL between 15 and 25 indicating A-4 samples matching the AHTD boring log data in Section 3.3. Often the LL in isolation is insufficient for distinguishing between clay and silt soils using AASHTO soil classification since both clay and silt samples have similar LL characteristics. The relationship between the soil properties and resistivity shown in Figure 4-2, Figure 4-3 and Figure 4-4 all reveal poor correlations which may be due to the difference in precipitation between the time the samples were tested and the time the CCR survey was conducted aligning with the concerns mentioned in Section 3.3.

The error distributions shown in Figure 4-2, Figure 4-3 and Figure 4-4 and calculated according to Equations 4.1-4.4 indicates 44% of the clay samples have resistivity values



greater than 150 ohm-m and 47% of the silt samples have resistivity values less than 150 ohm-m indicating large amounts of inaccurate clay and silt predictions using resistivity. The high error percentages indicate the inability of resistivity to separate clay and silt soils at this site. Analysis of soil sample distribution shown in Figure 4-5 reveals 95 percent of the AASHTO classified silt samples have resistivity values between 50 and 300 ohm-m, and 82% of the clay samples have resistivity values between 50 and 250 ohm-m. The observations from all the figures highlight the difficulty in separating clay and silt samples using resistivity, as there is little separation between them leading to the representation of most clay and silty samples within the resistivity range of 50 to 300 ohm-m in the dry conditions of Alpena, AR. The silty sand samples also fall within the resistivity range of clay and silt due to the silt content. The observations concerning the clay and silt samples are reflected in the soil range color map shown in Figure 4-1 where clay and silt are assigned a resistivity value of 300 ohm-m or less and bedrock is assigned resistivity values  $> 300$  ohm-m similar to the typical values established by Palacky. (1987), Burger et al. (1992), and Hickin et al. (2008).

In terms of predict fine grain soils (clay and silts) and course grained soils (sand and gravels), the estimated soil type from CCR matched the boring logs at 32 of the 36 sample locations indicating CCR had 90% accuracy for identifying course and fine grained soils at the Alpena site. The CCR method was able to provide an accurate analysis of locations believed to contain potential bedrock by providing a non-localized subsurface view from which a distinction between a rock fragment surrounded by fine grain soil, and extensive bedrock was possible. Although the CCR method is accurate enough for identifying fine grain soils, limitations exist in an inability to distinguishing between clay and silt.

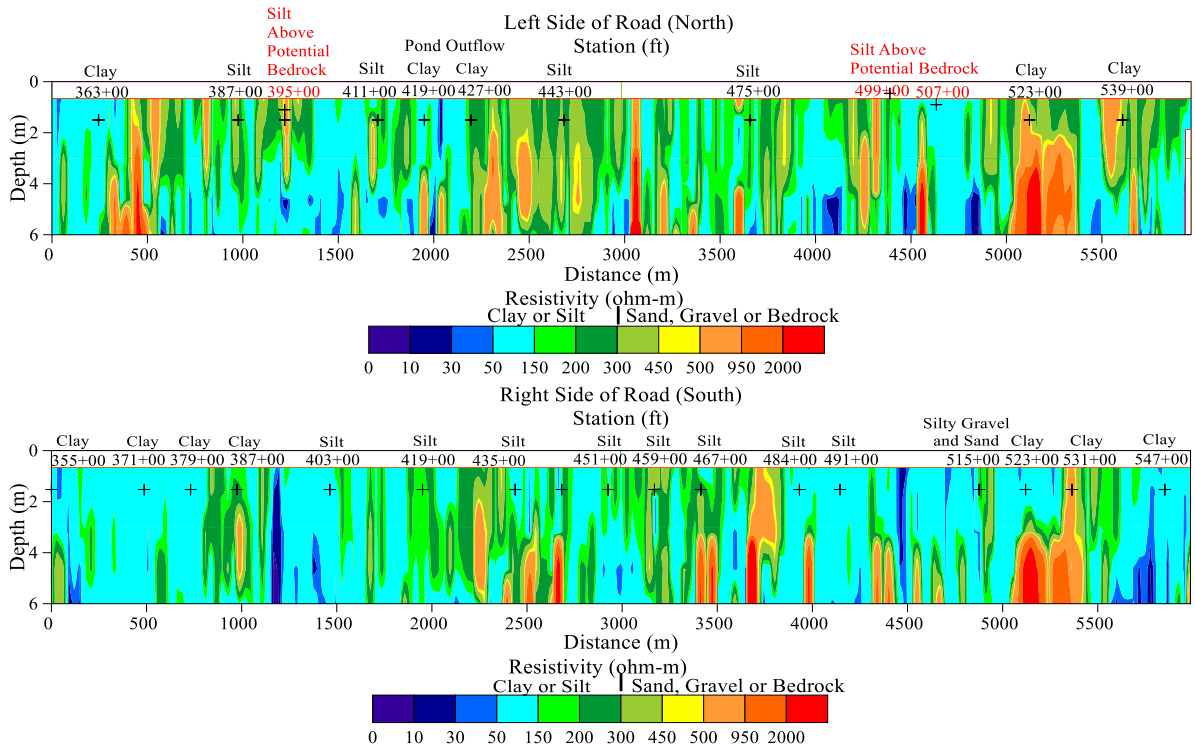


Figure 4-1. Resistivity soil profiles along the left and right side of the road at Alpena, Arkansas showing the soil type, station, and boring depth location at the top of the resistivity plot

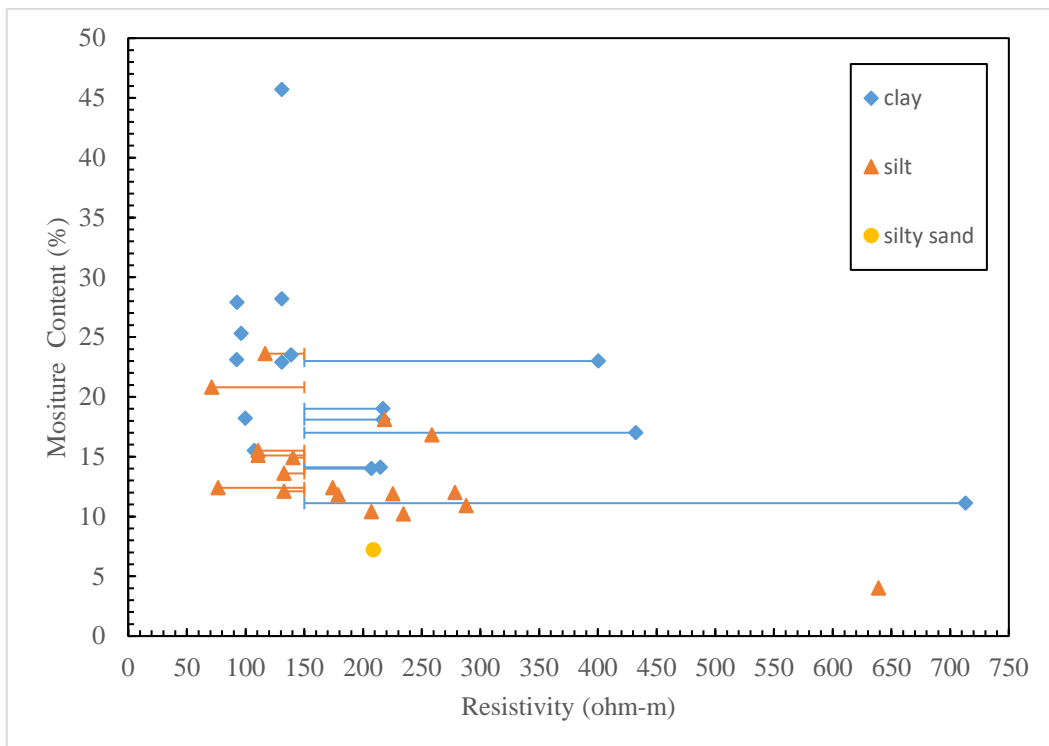


Figure 4-2. Relationship between moisture content and resistivity of boring log soil samples collected at the Alpena, Arkansas site.

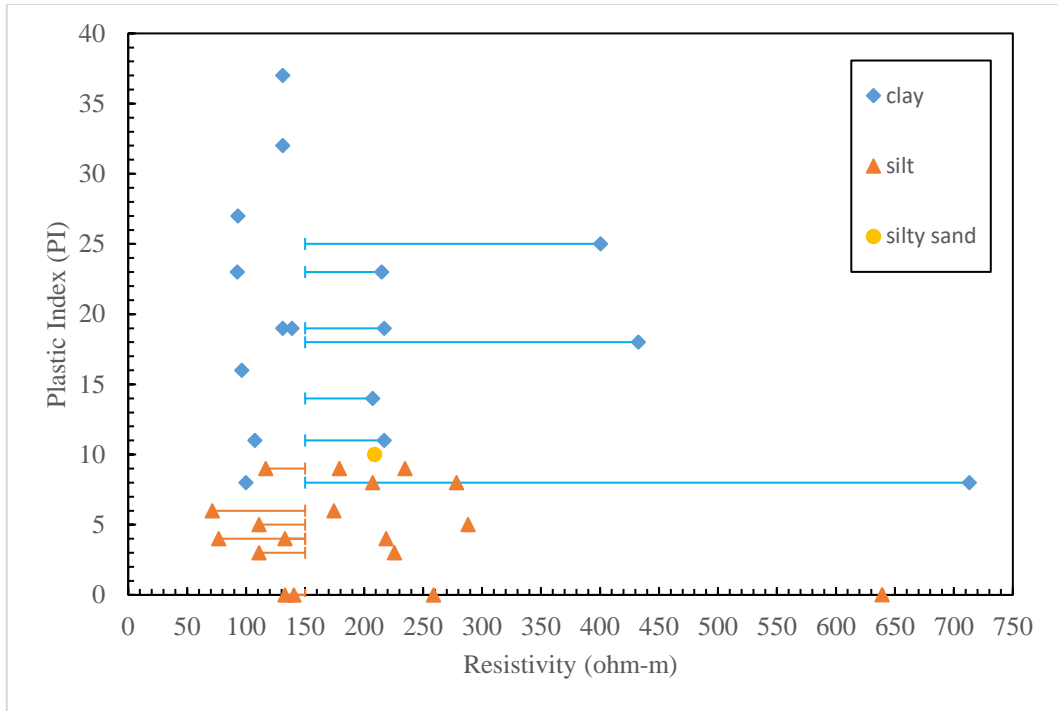


Figure 4-3. Relationship between plastic index and resistivity of boring log soil samples collected at the Alpena, Arkansas site.

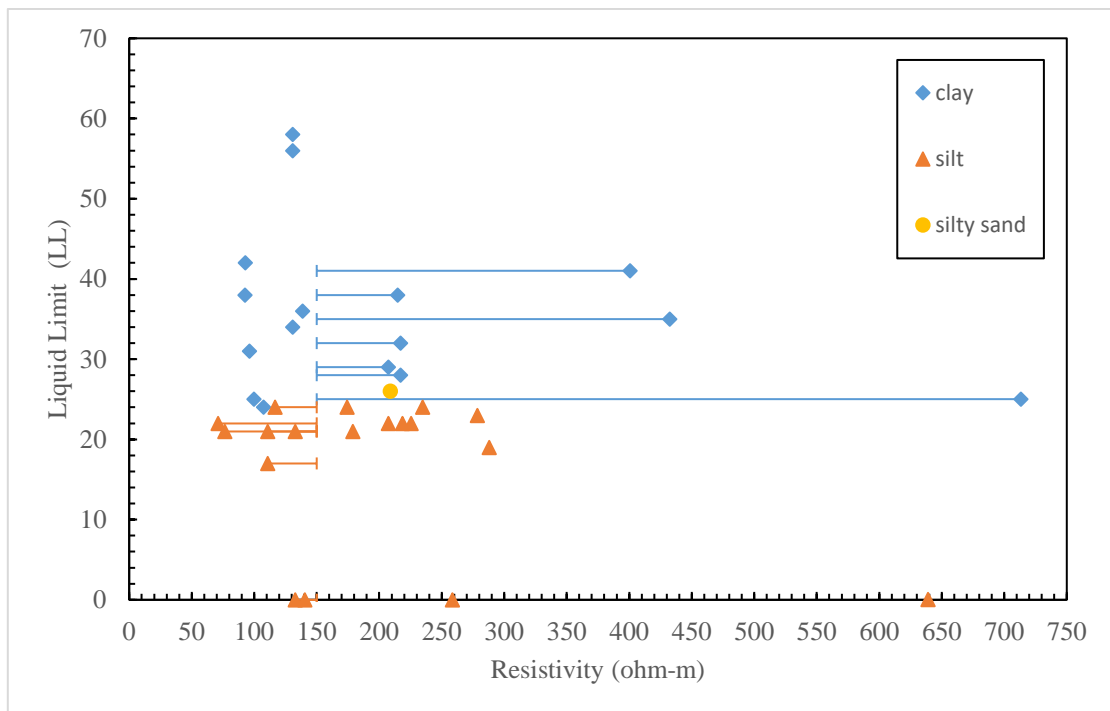


Figure 4-4. Relationship between liquid limit and resistivity of boring log soil samples collected at the Alpena, Arkansas site.

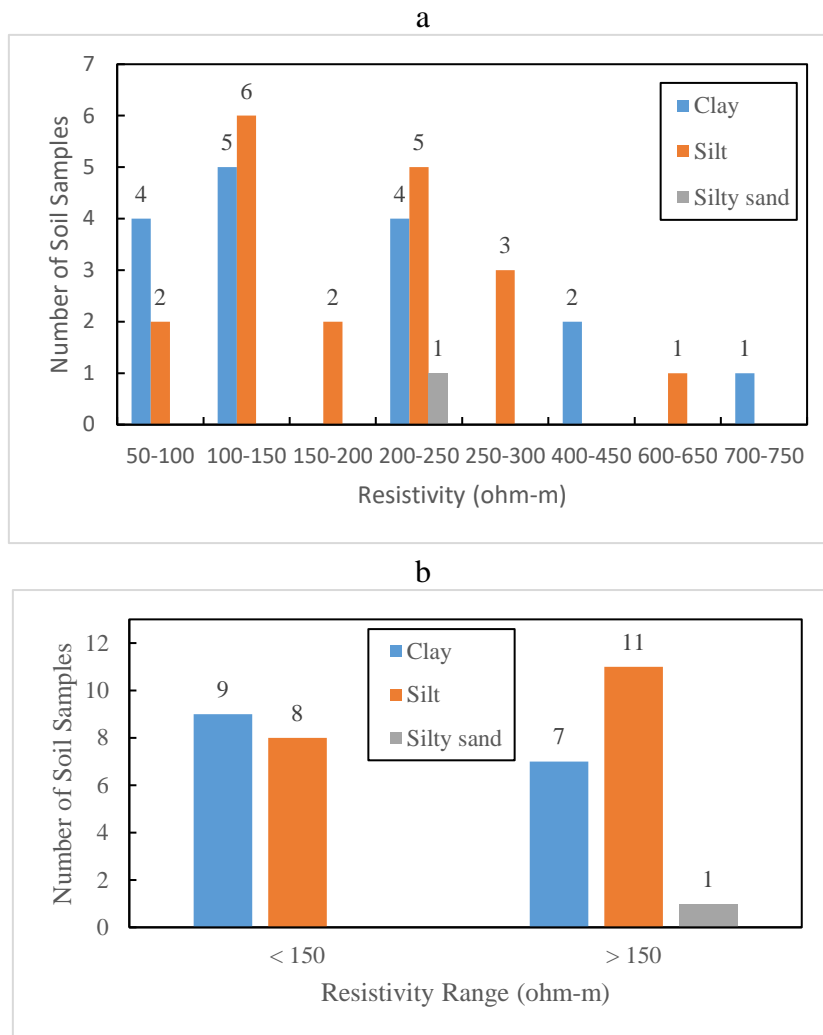


Figure 4-5. a) Distribution of soil samples for various resistivity values and b) Distribution of soil samples either side hypothetical resistivity separator between clay and silt samples based on resistivity at the Alpena site.

## 4.2 Mel Price Levee

### 4.2.1 Landside

The resistivity profile generated from the data acquired along the landside of the Mel Price Levee site is shown in Figure 4-6. The profile contains the boring log information at stations along the levee and reaches a maximum depth 10 meters below the surface. The resistivity profile is comprised of three layers of soil, which are clay (C), silty sand (SM) and sand (S) confirming the soil types and layers identified in the boring logs. Assigning the soils to resistivity ranges at this site was possible by aligning the results from the CCR data

processing with the existing boring log data. Resistivity values between 0-35 ohm-m indicate a clay layer at a depth of 0 to 2 meters, and greater than 35 ohm-m indicate a sandy layer at a depth of 2 to 10 meters comprised of silty sand and sand. No boring log information is available for the portion of the profile between Station 115+00 to 123+00 but the resistivity values reveal the presence of significant clay or low resistivity sand, which is a variation from the majority of the profile. In reality, the soil at this portion was highly saturated evident by the standing water noticed during the data collection process discussed in Section 3.4, which may have led to errors in the estimated resistivity.

The relationship between PI and resistivity is shown in Figure 4-7 for soil samples classified as clay and sand based on the Unified Soil Classification System (USCS) criteria. Soils samples are classified as fine-grained soils if 50% or more of the sample passed the No. 200 sieve and PI is greater than 0, or coarse-grained soils if more than 50% of the sample is retained on the No. 200 sieve and typically PI is 0.

The clay samples shown in Figure 4-7 have a PI greater than 5, and most sand samples have PI of 0 matching the USCS criteria for both soil types highlighting the role played by PI in USCS soil classification system. While resistivity does an acceptable job of separating the clay and sand soil samples, it does have some errors. Identifying the soil types based on resistivity is shown in Figure 4-8, where 88% of the clay samples have a maximum resistivity value of 35 ohm-m, and 90% of the sand samples have a minimum resistivity value of 35 ohm-m. The resistivity distribution of the soil samples indicates the effectiveness of separating clay and sand based on resistivity.

These values are noticeably less than the typical resistivity values and this can be attributed to the very high water level at the landside of the levee. Therefore, the standard resistivity ranges may not be applicable for all sites.

The soil types predicted using CCR failed to match the boring logs for just 10 of the 246 soil samples indicating the CCR method had 89% accuracy at separating clay and sand at the landside of Mel Price Levee. Although the CCR method displays considerable accuracy in distinguishing between fine and coarse grain soils, and predict the soil layers, it is susceptible to misinterpretation of the soil type caused by changes in water levels evident at a section along the landside of the levee. The CCR method is accurate enough for identifying soil types as long as water levels are monitored at the site.

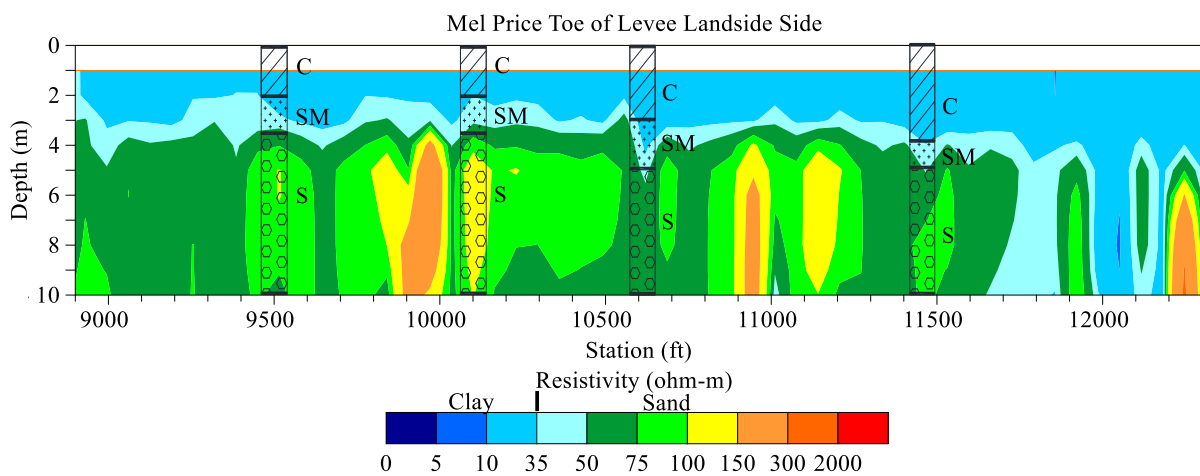


Figure 4-6. Resistivity profile from CCR along the landside of Mel Price Levee.

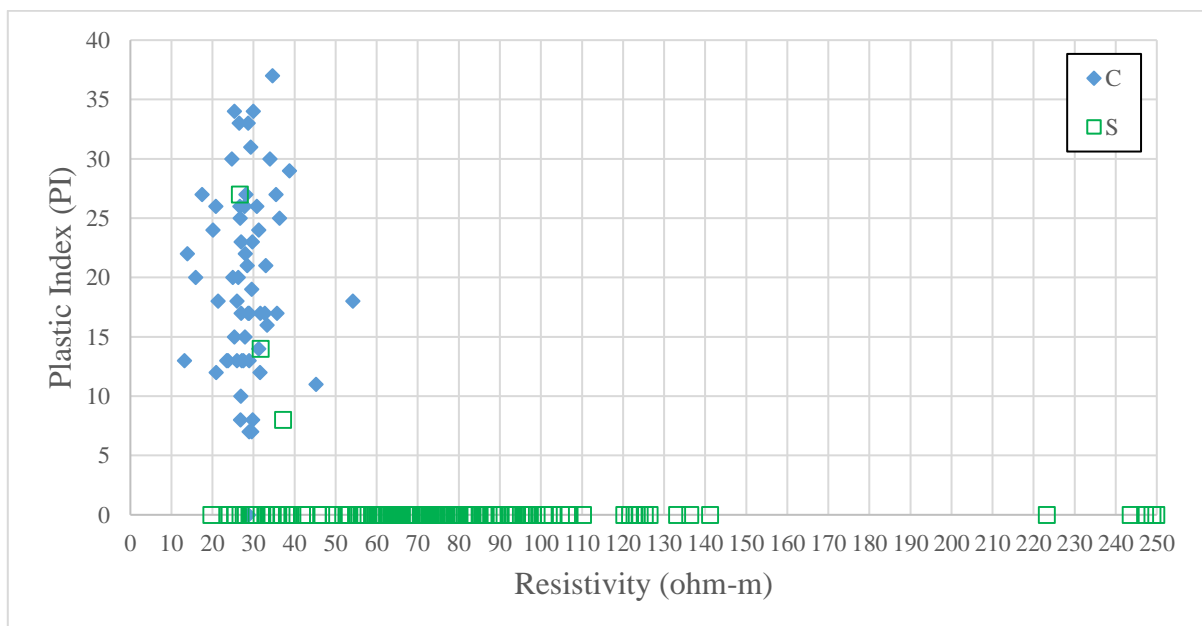


Figure 4-7. Plot of relationship between plastic index and resistivity of boring log soil samples collected along the landside of the Mel Price Levee.

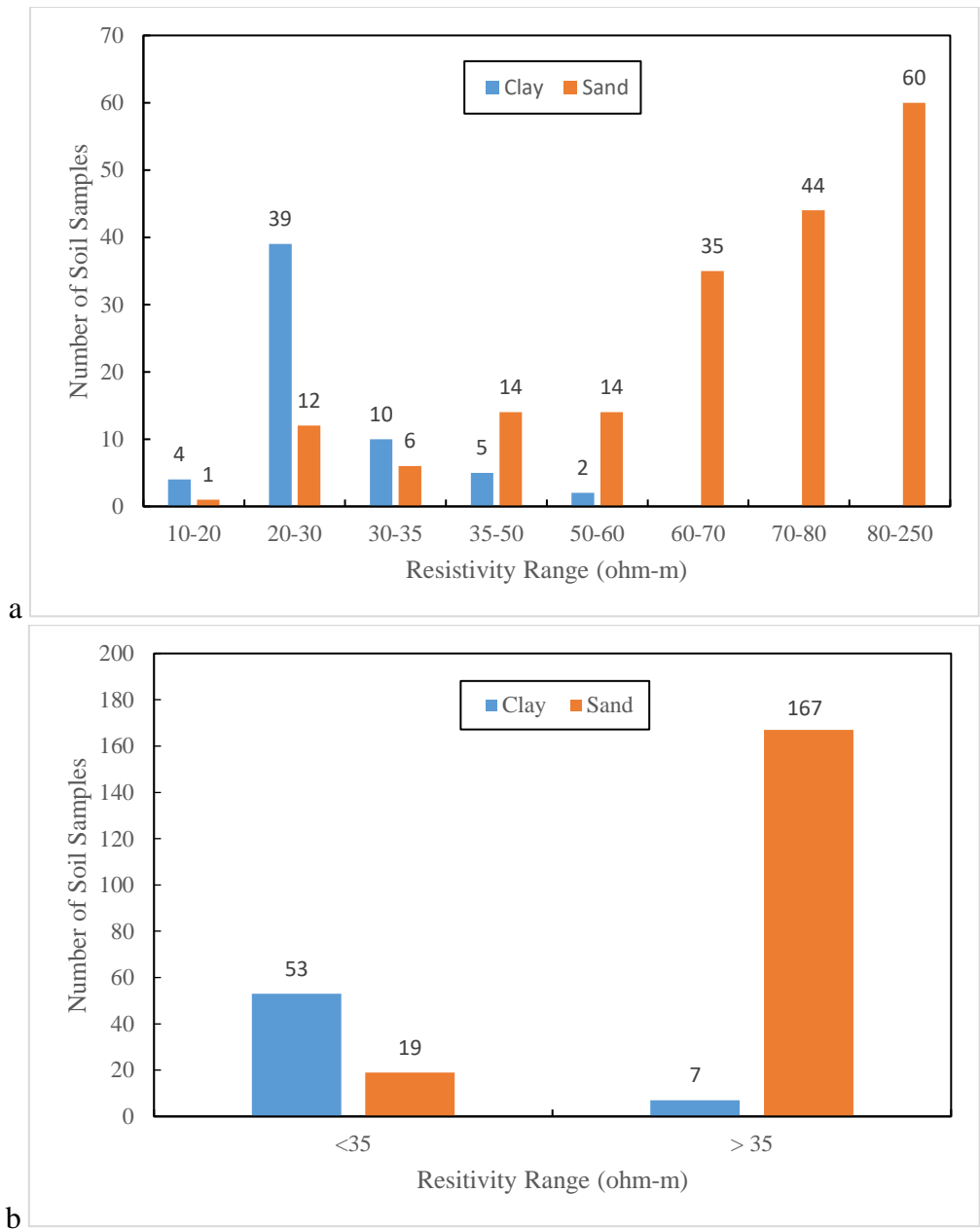


Figure 4-8. a) Distribution of soil samples b) Distribution of soil samples either side hypothetical resistivity separator between clay and sand samples based on their resistivity at landside of Mel Price site.

#### 4.2.2 Riverside

The resistivity profile generated from the data acquired along the riverside of the Mel Price Levee site is shown in Figure 4-9 and reaches a maximum depth 9 meters below the surface. The CPT cone resistance ( $q_c$ ), friction ratio ( $R_f$ ) and CPT sleeve friction ( $f_s$ ) values contained in the CPT logs for the Mel Price Levee site were used to estimate the subsurface soil types along the levee based on the soil behavior type ( $I_{SBT}$ ) relationships developed by

Robertson et al (2010). The results based on the  $I_{SBT}$  show the levee is comprised of clay and sand soil layers, distributed along the riverside as shown in Figure 4-9. The resistivity profile shows resistivity values between 0-40 ohm-m indicating a clay layer at depths of 0 to 2 meters, and greater than 40 ohm-m indicating sand layer at depths of 2 to 9 meters. The profile also shows sections along the levee where prior to the levee's construction were part of the Mississippi River. Those old river sections appear to have a lower resistivity than the other sections with naturally deposited soils along the levee due to the younger river deposits in the area.

The relationship between the soil behavior type ( $I_{SBT}$ ) and resistivity is shown in Figure 4-10 for the Mel Price Data. The  $I_{SBT}$  value of the sand samples are from 1.4 to 2.5, and clay samples are from 2.5 to 3.5. This verifies that the  $I_{SBT}$  was applied accurately to identify the soil types. The distribution of soil samples based on resistivity shown in Figure 4-11 indicates 80% of the clay samples have resistivity less than 40 ohm-m, and 88% of the sand samples have resistivity values greater than 40 ohm-m. This distribution shows that clay and sand samples can be separated adequately using resistivity. Similar to the landside, these values are much less than the typical resistivity values due to the high water content along the riverside of the levee. The resistivity separation point between the clay and sand at the riverside of the levee is 40 ohm-m, a slightly greater value than the 35 ohm-m identified at the landside. This slight difference could also be attributed to the difference in water level along both sides of the levee.

The soil types predicted using CCR failed to match the results from the CPT logs at 9 of the 58 station depths with recorded CPT data indicating CCR had an 84% accuracy for identify clay and sand along the riverside of the levee. Although CCR displays considerable accuracy for distinguishing between layers of fine and coarse grain soil, it is susceptible to misinterpretation of the soil type caused by changes in soil deposition at sections along the



riverside of the levee that alter the resistivity values.

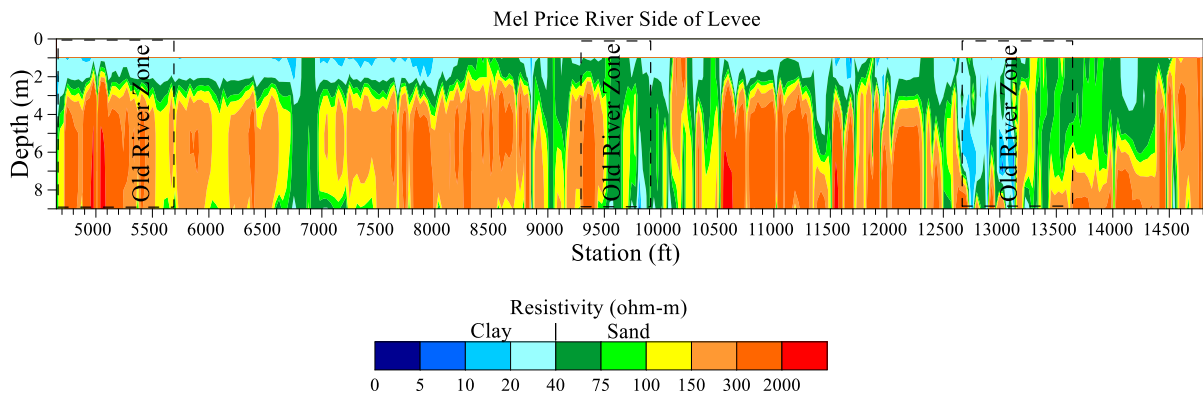


Figure 4-9. Resistivity profile from CCR along the riverside of Mel Price Levee.

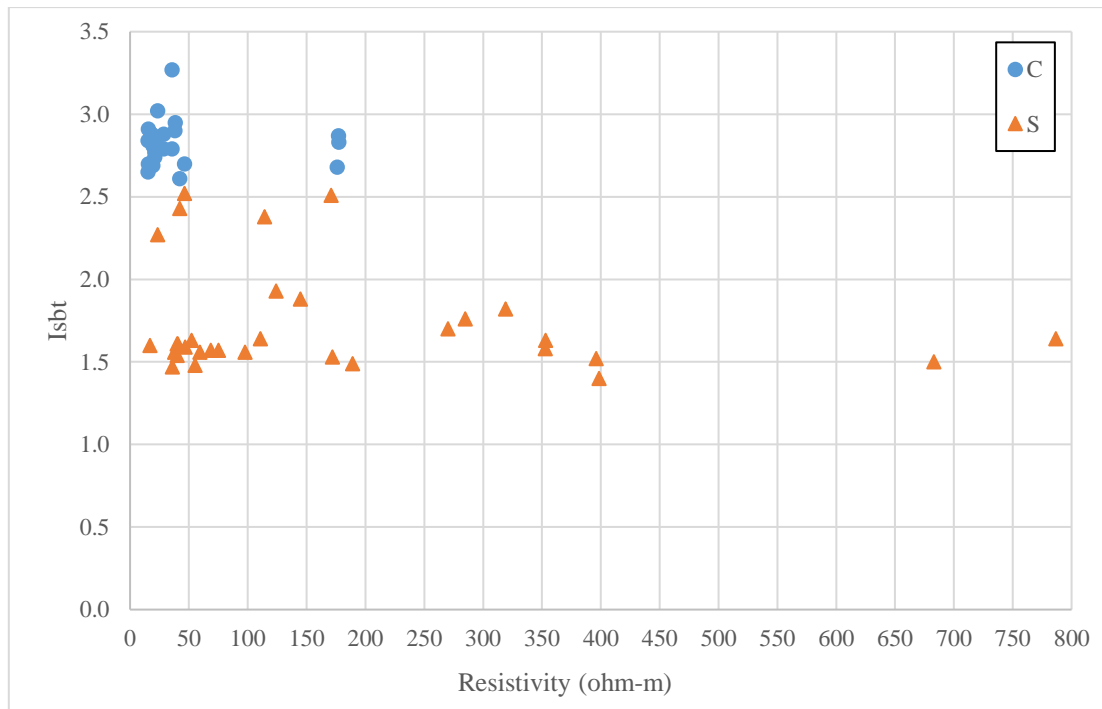


Figure 4-10. Relationship between  $I_{sbt}$  and resistivity of CPT soil samples collected along the riverside of the Mel Price Levee. Identified soil types are based on  $I_{sbt}$ .

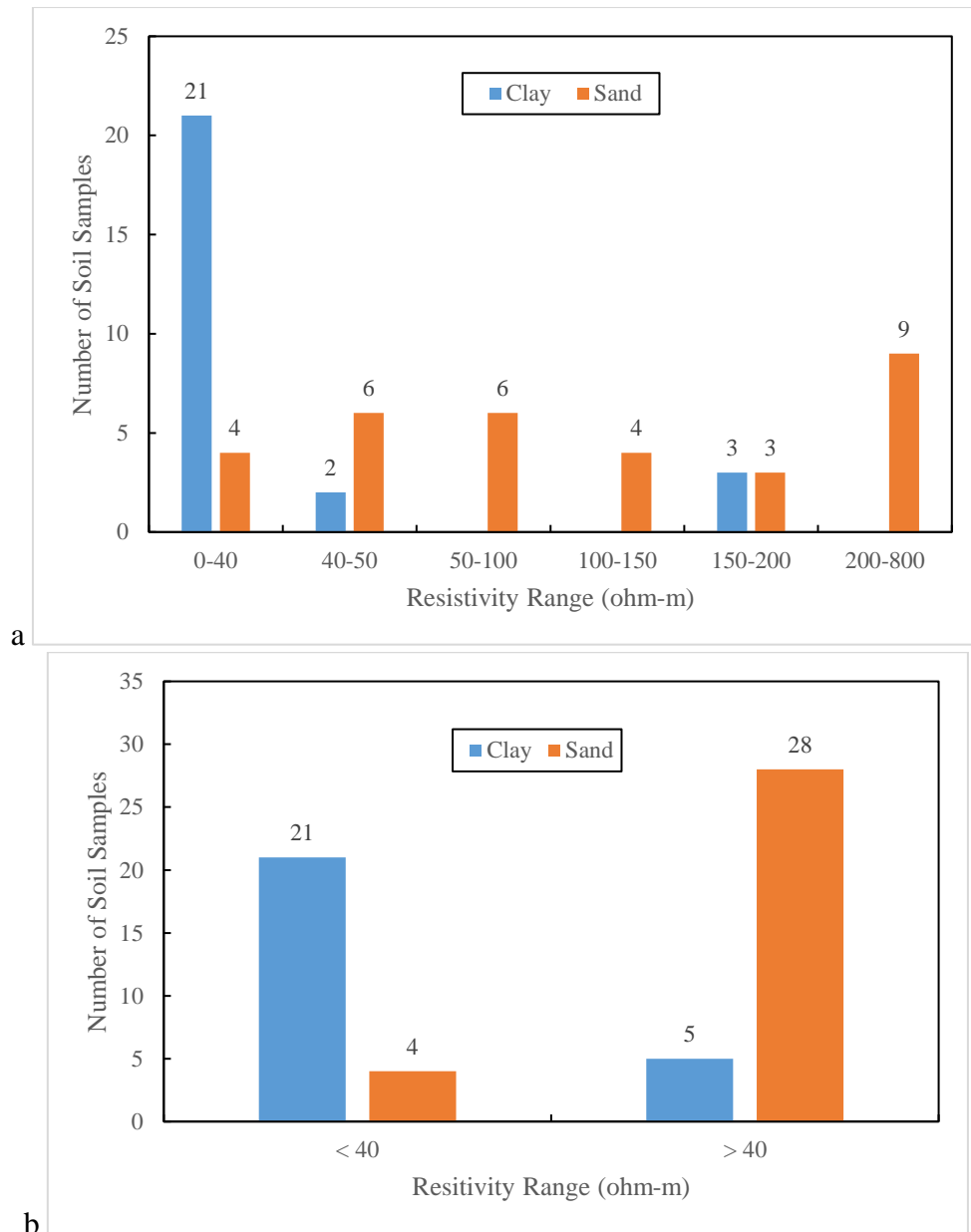


Figure 4-11. a) Distribution of soil samples b) Distribution of soil samples either side of a hypothetical resistivity separator between clay and sand samples based on their resistivity along the riverside of Mel Price Levee.

#### 4.2.3 Comparison between Resistivity Results

The resistivity profile for Alpena indicates the subsurface is composed of mostly clay and silt soil layers and based on their resistivity values both soil layers are nearly indistinguishable falling within the same resistivity range as shown in Table 4-1. The layering for the Mel Price Levee indicates the subsurface is composed of clay and sand soil layers and based on their resistivity values both are separable falling within different resistivity ranges as shown in Table 4-1. The resistivity values measured at the Alpena site were much less than

those measured at the Mel Price Levee and this can be attributed to the difference in water level observed at both sites with Alpena having a deep water table and Mel Price Levee having a shallow water table. Table 4-1 shows that the resistivity ranges for the dry soils at the Alpena site, and the wet soils at the Alton site have similar resistivity values with the dry and wet subsurface soils surveyed by Hayashi et al. (2010), Gun et al. (2015), Garman et al. (2004), and Keller & Frischknecht. (1966).

Table 4-1. Resistivity soil ranges from the Alpena, AR, Alton, IL sites, and other resistivity tests by Hayashi et al. (2010), Gun et al. (2015), Garman et al. (2004), and Keller & Frischknecht. (1966).

Soil	Resistivity (ohm-m)						
	Alpena, AR	Alton, IL Landside	Alton, IL Riverside	Hayashi et al. 2010 Riverside	Gun et al. 2015	Garman et al. 2004	Keller & Frischknecht. 1966
	Dry Soil	Wet Soil	Wet Soil	Wet Soil	Wet Soil	Dry Soil	Wet Soil
Clay and Silty Sand	0 - 300	0 - 50	0 - 40	0 - 80	0 - 150	0 - 500	0 to 100
Sand, Gravel, Bedrock	> 300	> 50	> 40	> 80	> 150	> 500	> 100

## 5 Conclusion

Subsurface soil investigation conducted using traditional drilling and sampling methods provide data at only discrete locations. The CCR survey performed at sites in Alpena, AR and Alton, IL provided uniform data of the subsurface demonstrating an improvement on the traditional methods. Localized changes in stratigraphy were evident at both sites, but the results of the CCR survey revealed the current limitations of this method.

CCR can distinguish between fine-grained soil and coarse grain soils, but unlike traditional methods, it cannot distinguish between clay and silt both of which are fine-grained soils. The results also show that low and high plasticity fine-grained soils exist within the same resistivity ranges highlighting the inability of CCR to make a distinction based on plasticity unlike traditional methods that for example can distinguish between CH and CL.

The level of the water table at both sites had an impact on the observed soil resistivity ranges. The water table was deep at the Alpena site resulting in dry conditions, while the water table was shallow at the Alton site resulting in wet conditions. The fine-grained soil had a resistivity range of 0-300 ohm-m at the dry conditions of Alpena, and 0-50 ohm-m at the wet conditions of Alton indicating that soil resistivity reduces as the subsurface soil becomes saturated. The method of soil deposition had an impact on the resistivity values at a section along the Mel Price Levee where prior to the levee's construction was part of a river channel. The resistivity values at that section were less than the other sections with naturally deposited soils that predated the levee's construction.

The soil resistivity ranges were initially developed using existing values from preexisting resistivity tests then adjusted to match the soil predictions in the existing boring and CPT logs. The dependence of soil resistivity ranges on traditional methods indicates that presently the CCR methods alone is incapable of accurately predicting subsurface stratigraphy if moisture conditions are unknown. This dependence can be reduced by further CCR research being performed with increased importance attributed to site conditions such as water level and method of soil deposition at the test sites creating a library of knowledge from which the parameters that affect soil resistivity can be better understood establishing strong correlations.

## **6 References**

- Allred, B. J., Ehsani, M. R., & Saraswat, D. (2006). Comparison of electromagnetic induction, capacitively-coupled resistivity, and galvanic contact resistivity methods for soil electrical conductivity measurement. *Applied engineering in agriculture*, 22(2), 215-230.
- Asch, T. H., Deszcz-Pan, M., Burton, B. L., & Ball, L. B. (2008). *Geophysical Characterization of the American River Levees, Sacramento, California, using Electromagnetics, Capacitively Coupled Resistivity, and DC Resistivity*. U. S. Geological Survey.
- Burger, H.R. (1992). *Exploration Geophysics of the Shallow Subsurface*. Prentice-Hall, Englewood Cliffs, NJ, 489.

- Burton, B. L., & Cannia, J. C. (2011). *Capacitively coupled resistivity survey of the levee surrounding the Omaha Public Power District Nebraska City Power Plant, June 2011*. US Department of the Interior, US Geological Survey.
- Cardarelli, E., Cercato, M., & De Donno, G. (2014). Characterization of an earth-filled dam through the combined use of electrical resistivity tomography, P- and SH-wave seismic tomography and surface wave data. *Journal of Applied Geophysics*, 106, 87-95.
- Dahlin, T. (1996). 2D resistivity surveying for environmental and engineering applications. *First break*, 14(7), 275-283.
- deGroot-Hedlin, C., & Constable, S. (1990). Occam's inversion to generate smooth, two-dimensional models from magnetotelluric data. *Geophysics*, 55(12), 1613-1624.
- Gunn, D. A., Chambers, J. E., Uhlemann, S., Wilkinson, P. B., Meldrum, P. I., Dijkstra, T. A., ... & Hughes, P. N. (2015). Moisture monitoring in clay embankments using electrical resistivity tomography. *Construction and Building Materials*, 92, 82-94.
- Garman, K. M., & Purcell, S. F. (2004). Applications for capacitively coupled resistivity surveys in Florida. *The Leading Edge*, 23(7), 697-698.
- Geometrics, 2007, OhmMapper Capacitively Coupled Resistivity System: <http://www.geometrics.com/OhmMapper/>
- Hayashi, K., & Konishi, C. (2010). Joint use of a surface-wave method and a resistivity method for safety assessment of levee systems. In *GeoFlorida 2010: Advances in Analysis, Modeling & Design* (pp. 1340-1349).
- Hickin, A. S., Kerr, B., Barchyn, T. E., & Paulen, R. C. (2009). Using ground-penetrating radar and capacitively coupled resistivity to investigate 3-D fluvial architecture and grain-size distribution of a gravel floodplain in northeast British Columbia, Canada. *Journal of Sedimentary Research*, 79(6), 457-477.
- Keller, G. V., & Frischknecht, F. C. (1966). *Electrical methods in geophysical prospecting*.
- Kuras, O. (2002). *The capacitive resistivity technique for electrical imaging of the shallow subsurface* (Doctoral dissertation, University of Nottingham).
- Loke, M. H. (2003). Rapid 2D Resistivity & IP Inversion using the least-squares method. *Geotomo Software. Manual*.
- Lucius, J. E., Abraham, J. D., & Burton, B. L. (2008). *Resistivity Profiling for Mapping Gravel Layers that may Control Contaminant Migration at the Amargosa Desert Research Site, Nevada* (No. 2008-5091). Geological Survey (US).
- Palacky, G.J., 1987. Clay mapping using electromagnetic methods. *First Break* 5, 295–306.
- Rahimi, S., Wood, C. Folaseye, C., Moody, T., Bernhardt-Barry, M., Mofarraj Kouchaki, B., (2018). The Combined Use of MASW and Resistivity Surveys for Levee Assessment: A Case Study of the Melvin Price Reach of the Wood River Levee, *Engineering Geology*. (<https://doi.org/10.1016/j.enggeo.2018.05.009>).
- Robertson, P. K. (2010, May). Soil behaviour type from the CPT: an update. In *2nd international symposium on cone penetration testing, USA* (pp. 9-11).

Sabo, S. H. (2008). *Evaluation of capacitively-coupled electrical resistivity for locating solution cavities overlain by clay-rich soils* (Doctoral dissertation, Bowling Green State University).

Samouëlian, A., Cousin, I., Tabbagh, A., Bruand, A., & Richard, G. (2005). Electrical resistivity survey in soil science: a review. *Soil and Tillage research*, 83(2), 173-193.

Sudha, K., Israil, M., Mittal, S., & Rai, J. (2009). Soil characterization using electrical resistivity tomography and geotechnical investigations. *Journal of Applied Geophysics*, 67(1), 74-79.

Vadillo, I., Benavente, J., Neukum, C., Grützner, C., Carrasco, F., Azzam, R., ... & Reicherter, K. (2012). Surface geophysics and borehole inspection as an aid to characterizing karst voids and vadose ventilation patterns (Nerja research site, S. Spain). *Journal of Applied Geophysics*, 82, 153-162.

Walker, J. P., & Houser, P. R. (2002). Evaluation of the OhmMapper instrument for soil moisture measurement. *Soil Science Society of America Journal*, 66(3), 728-734.